

1  
2 **A Phenomenology of New Particle Formation (NPF) at**  
3 **Thirteen European Sites**  
4

5 **Dimitrios Bousiotis<sup>1</sup>, Francis D. Pope<sup>1</sup>, David C. Beddows<sup>1</sup>,**  
6 **Manuel Dall'Osto<sup>2</sup>, Andreas Massling<sup>3</sup>, Jacob Klenø Nøjgaard<sup>3,4</sup>,**  
7 **Claus Nordstrøm<sup>3</sup>, Jarkko V. Niemi<sup>5</sup>, Harri Portin<sup>5</sup>, Tuukka Petäjä<sup>6</sup>,**  
8 **Noemi Perez<sup>7</sup>, Andrés Alastuey<sup>7</sup>, Xavier Querol<sup>7</sup>, Giorgos Kouvarakis<sup>8</sup>,**  
9 **Stergios Vratolis<sup>9</sup>, Konstantinos Eleftheriadis<sup>9</sup>, Alfred Wiedensohler<sup>10</sup>,**  
10 **Kay Weinhold<sup>10</sup>, Maik Merkel<sup>10</sup>, Thomas Tuch<sup>10</sup> and Roy M. Harrison<sup>1\*†</sup>**  
11

12 **<sup>1</sup>Division of Environmental Health and Risk Management**  
13 **School of Geography, Earth and Environmental Sciences**  
14 **University of Birmingham, Edgbaston, Birmingham B15 2TT, United Kingdom**  
15

16 **<sup>2</sup>Institute of Marine Sciences**  
17 **Passeig Marítim de la Barceloneta, 37-49, E-08003, Barcelona, Spain**  
18

19 **<sup>3</sup>Department of Environmental Science, Aarhus University, 4000 Roskilde, Denmark**  
20

21 **<sup>4</sup>The National Research Centre for the Working Environment, 2100 Copenhagen, Denmark**  
22

23 **<sup>5</sup>Helsinki Region Environmental Services Authority (HSY),**  
24 **FI-00066 HSY, Helsinki, Finland**  
25

26 **<sup>6</sup>Institute for Atmospheric and Earth System Research (INAR) / Physics, Faculty of Science,**  
27 **University of Helsinki, Finland**  
28

29 **<sup>7</sup>Institute of Environmental Assessment and Water Research (IDAEA - CSIC), 08034,**  
30 **Barcelona, Spain**  
31

32 **<sup>8</sup>Environmental Chemical Processes Laboratory (ECPL), Department of Chemistry,**  
33 **University of Crete, 70013, Heraklion, Greece**

---

\* To whom correspondence should be addressed (Email: [r.m.harrison@bham.ac.uk](mailto:r.m.harrison@bham.ac.uk))

†Also at: Department of Environmental Sciences / Center of Excellence in Environmental Studies, King Abdulaziz University, PO Box 80203, Jeddah, 21589, Saudi Arabia

34  
35  
36  
37  
38  
39  
40  
41  
42

**<sup>9</sup>Environmental Radioactivity Laboratory, Institute of Nuclear and Radiological Science & Technology, Energy & Safety, NCSR Demokritos, Athens, Greece**

**<sup>10</sup>Leibniz Institute for Tropospheric Research (TROPOS),  
Permoserstr. 15, 04318 Leipzig, Germany**

## 43 **ABSTRACT**

44 New particle formation (NPF) events occur almost everywhere in the world and can play an  
45 important role as a particle source. The frequency and characteristics of NPF events vary spatially  
46 and this variability is yet to be fully understood. In the present study, long term particle size  
47 distribution datasets (minimum of three years) from thirteen sites of various land uses and climates  
48 from across Europe were studied and NPF events, deriving from secondary formation and not  
49 traffic related nucleation, were extracted and analysed. The frequency of NPF events was  
50 consistently found to be higher at rural background sites, while the growth and formation rates of  
51 newly formed particles were higher at roadsides (though in many cases differences between the  
52 sites were small), underlining the importance of the abundance of condensable compounds of  
53 anthropogenic origin found there. The growth rate was higher in summer at all rural background  
54 sites studied. The urban background sites presented the highest uncertainty due to greater variability  
55 compared to the other two types of site. The origin of incoming air masses and the specific  
56 conditions associated with them greatly affect the characteristics of NPF events. In general, cleaner  
57 air masses present higher probability for NPF events, while the more polluted ones show higher  
58 growth rates. However, different patterns of NPF events were found even at sites in close proximity  
59 (< 200 km) due to the different local conditions at each site. Region-wide events were also studied  
60 and were found to be associated with the same conditions as local events, although some variability  
61 was found which was associated with the different seasonality of the events at two neighbouring  
62 sites. NPF events were responsible for an increase in the number concentration of ultrafine particles

63 of more than 400% at rural background sites on the day of their occurrence. The degree of  
64 enhancement was less at urban sites due to the increased contribution of other sources within the  
65 urban environment. It is evident that, while some variables (such as solar radiation intensity,  
66 relative humidity or the concentrations of specific pollutants) appear to have a similar influence on  
67 NPF events across all sites, it is impossible to predict the characteristics of NPF events at a site  
68 using just these variables, due to the crucial role of local conditions.

69

70 **Keywords:** Nucleation; New Particle Formation; Ultrafine Particles; Roadside; Urban Background;

71 Rural

72

## 73 **1. INTRODUCTION**

74 Ultrafine particles (particles with diameter smaller than 100 nm), while not yet regulated, are  
75 believed to have adverse effects upon air quality and public health (Atkinson et al., 2010; Politis et  
76 al., 2008; Tobías et al., 2018), as well as having a direct or indirect effect on atmospheric properties  
77 (Makkonen et al., 2012; Seinfeld and Pandis, 2012). The source of ultrafine particles can either be  
78 from primary emissions (Harrison et al., 2000; Masiol et al., 2017), including delayed primary  
79 emissions (Hietikko et al., 2018; Olin et al., 2020; Rönkkö et al., 2017), or from secondary  
80 formation from gaseous precursors (Brean et al., 2019; Chu et al., 2019; Kerminen et al., 2018;  
81 Kulmala et al., 2004a; Yao et al., 2018), which is considered as an important source of CCN in the  
82 atmosphere (Dameto de España et al., 2017; Kalivitis et al., 2015; Spracklen et al., 2008). For the  
83 latter, while the process of formation of initial clusters that subsequently lead to particle formation  
84 has been extensively studied (Dal Maso et al., 2002; Kulmala et al., 2014; Riipinen et al., 2007;  
85 Weber et al., 1998), there is no consistent explanation of the factors which determine the occurrence  
86 and development of NPF events in the atmosphere. Additionally, events that resemble NPF, with  
87 the initial particles deriving from primary emissions, especially close to traffic sources (Rönkkö et  
88 al., 2017), have been also reported but these are out of the scope of the present study.

89

90 A large number of studies both in laboratories and in real world conditions have been conducted to  
91 either describe or explain the mechanisms that drive NPF events. The role of meteorological  
92 conditions, such as solar radiation intensity (Kumar et al., 2014; Shi et al., 2001; Stanier et al.,

93 2004) and relative humidity (Li et al., 2019; Park et al., 2015), are well documented, while great  
94 diversity was found for the effect of other meteorological factors such as the wind speed (Charron et  
95 al., 2008; Németh and Salma, 2014; Rimnácová et al., 2011) or temperature (Jeong et al., 2010;  
96 Napari et al., 2002). There are also influences of atmospheric composition, with the positive role of  
97 low condensation sink and concentrations of pollutants such as NO<sub>x</sub> upon NPF event occurrence  
98 being widely agreed upon (Alam et al., 2003; Cheung et al., 2013; Kerminen et al., 2004; Wang et  
99 al., 2014; Wehner et al., 2007). Contrary to that, while the indirect role of SO<sub>2</sub> is well established in  
100 the nucleation process, via the formation of new clusters of H<sub>2</sub>SO<sub>4</sub> molecules (Boy et al., 2005; Iida  
101 et al., 2008; Kulmala et al., 2005; Sipila et al., 2010; Xiao et al., 2015), uncertainty exists in the role  
102 that different concentrations of SO<sub>2</sub> play in the occurrence of NPF events in real world atmospheric  
103 conditions (Alam et al., 2003; Dall'Osto et al., 2018; Wonaschütz et al., 2015; Woo et al., 2001).  
104 Ammonia is known to enhance the formation of initial clusters (Korhonen et al., 1999; Ortega et al.,  
105 2008; Schobesberger et al., 2015), and volatile organic compounds are regarded as the main drivers  
106 of the growth of the newly formed particles (Kulmala et al., 2013; Riccobono et al., 2014; Tröstl et  
107 al., 2016). NPF events in different locations do not appear to follow consistent trends with the  
108 concentrations of these compounds and meteorological parameters (McFiggans et al., 2019;  
109 Minguillón et al., 2015; Riipinen et al., 2007), though links between NPF events and sulphuric acid  
110 vapour concentrations (Petäjä et al., 2009; Weber et al., 1995) and organics (Bianchi et al., 2019;  
111 Ehn et al., 2014) have been reported.

112

113 It is evident that NPF events and their development are complex, and local conditions play an  
114 important role in their variability. Many studies have attempted to explain this variability by  
115 analyzing multiple datasets from wider areas. Studies in the UK (Bousiotis et al., 2019; Hama et al.,  
116 2017), Spain (Brines et al., 2014; Carnerero et al., 2018; Dall'Osto et al., 2013; Minguillón et al.,  
117 2015), Hungary (Németh and Salma, 2014; Salma et al., 2014, 2016), Greece (Kalkavouras et al.,  
118 2017; Siakavaras et al., 2016), Germany (Costabile et al., 2009; Ma and Birmili, 2015; Sun et al.,  
119 2019) and China (Peng et al., 2017; Shen et al., 2018; Wang et al., 2017) have attempted to explain  
120 the differences found in NPF event conditions and variability between different sites in close  
121 proximity, while larger scale studies using descriptive (Brines et al., 2015; Hofman et al., 2016;  
122 Jaatinen et al., 2009; Kulmala et al., 2005) or statistical methods (Dall'Osto et al., 2018; Rivas et  
123 al., 2020) have provided insights into the effect of the variability of parameters that are considered  
124 to play an important role in the occurrence and development of NPF events on a broader scale.

125

126 The present study, combining thirteen long term datasets (minimum of three years) from different  
127 countries across Europe and combined with the results from a previous study in the UK, attempts to  
128 elucidate the effect of the local conditions on NPF event characteristics (frequency of NPF events,  
129 formation rate and growth rate) both for sites in close proximity (< 200 km), and by  
130 intercomparison of sites on a continental scale in order to find general trends of the variables that  
131 affect the characteristics and development of NPF events on a larger scale. Finally, the effect of

132 NPF events upon the ultrafine particle number concentrations was calculated, providing insight to  
133 the potential of NPF events to influence the local air quality conditions in all areas studied.

134

## 135 **2. DATA AND METHODS**

### 136 **2.1 Site Description and Data Availability**

137 In the present study, particle number size distribution data from 13 sites in Europe (Figure 1) are  
138 analysed in the size range  $3 \text{ nm} < D_p < 1000 \text{ nm}$ . A detailed list of the site locations and the data  
139 available for each is found in Table 1 (seasonal data availability is found in Table S1). For site naming  
140 the first three letters refer to the country (DEN = Denmark, GER = Germany, FIN = Finland, SPA =  
141 Spain, GRE = Greece) while the next two refer to the type of site (RU = Rural background, UB =  
142 Urban background, RO = Roadside). Average meteorological conditions and concentrations of  
143 chemical compounds for all sites are found in Tables S2 and S3 respectively; their seasonal variation  
144 is found in Table S4.

145

### 146 **2.2 Methods**

#### 147 **2.2.1 NPF event selection**

148 The identification of NPF events was conducted manually using the criteria set by Dal Maso et al.  
149 (2005). According to these, a NPF event is considered to occur when:

- 150 • a distinctly new mode of particles appears in the nucleation range,
- 151 • this new mode prevails for some hours,



152 • the new mode shows signs of growth.

153

154 The NPF events extracted using this method are then classified into classes I or II depending on the  
155 level of confidence. Class I (high confidence) is further classified as Ia and Ib, with class Ia  
156 containing the events that both present a clear formation of a new mode as well as a distinct growth  
157 of this mode, while Ib includes those with a less distinct formation and development. In the present  
158 study, only the events classified as Ia were used as they are considered as more suitable for study.  
159 As the growth criterion is not fully defined, in the present study a minimum growth rate of  $1 \text{ nm h}^{-1}$   
160 is required for NPF events to be considered. The events found using this method should not be  
161 confused with the formation and growth of particles deriving from primary emissions next to  
162 pollution sources, such as traffic. While to an extent the particle formation found can be biased by  
163 primary emissions (especially at roadside sites), great effort was made using additional data, such as  
164 atmospheric composition data, to not include any incidents of traffic related nucleation.

165

### 166 **2.2.2 Calculation of condensation sink, growth rate, formation rate, Nucleation Strength** 167 **Factor (NSF) and NPF event probability**

168 The calculation of the condensation sink was made using the method proposed by Kulmala et al.  
169 (2001). The condensation sink (CS) is calculated as:

170

$$171 \text{ CS} = 4\pi D_{vap} \sum \beta_M r N$$

172 where  $r$  and  $N$  are the radius and the number concentration of the particles and  $D_{\text{vap}}$  is the diffusion  
173 coefficient, calculated for  $T = 293$  K and  $P = 1013.25$  mbar, according to Poling et al. (2001):

174

$$175 \quad D_{\text{vap}} = 0.00143 \cdot T^{1.75} \frac{\sqrt{M_{\text{air}}^{-1} + M_{\text{vap}}^{-1}}}{P \left( D_{\text{x,air}}^{\frac{1}{3}} + D_{\text{x,vap}}^{\frac{1}{3}} \right)^2}$$

176

177 where  $M$  and  $D_x$  are the molar mass and diffusion volume for air and  $\text{H}_2\text{SO}_4$ .  $\beta_M$  is the Fuchs  
178 correction factor calculated from Fuchs and Sutugin (1971):

179

$$180 \quad \beta_M = \frac{1 + K_n}{1 + \left( \frac{4}{3a} + 0.377 \right) K_n + \frac{4}{3a} K_n^2}$$

181

182  $K_n$  is the Knudsen number, defined as  $K_n = 2\lambda_m/d_p$ , with  $\lambda_m$  being the mean free path of the gas.

183

184 The growth rate of the newly formed particles is calculated according to Kulmala et al. (2012), as

185

$$186 \quad \text{GR} = \frac{D_{P_2} - D_{P_1}}{t_2 - t_1}$$

187

188 for the size range between the minimum available particle diameter up to 30 nm. For the calculation  
 189 of the growth rate, the time considered was from the start of the event until a) growth stopped, b)  
 190 GMD reached the upper limit set or c) the day ended. Due to the differences in the smallest particle  
 191 size available between the sites, a discrepancy would exist for the growth rate values presented  
 192 (sites with lower size cut would present lower values of growth rate, as the growth rate tends to  
 193 increase with particle size in this range (Deng et al., 2020)). As a result, a direct comparison of the  
 194 growth rate values found among sites with significant differences at the smallest particle size  
 195 available was avoided.

196

197 The formation rate J was calculated using the method proposed by Kulmala et al. (2012) in which:

198

$$199 \quad J_{d_p} = \frac{dN_{d_p}}{dt} + \text{CoagS}_{d_p} \times N_{d_p} + \frac{\text{GR}}{\Delta d_p} \times N_{d_p} + S_{\text{losses}}$$

200

201 where  $\text{CoagS}_{d_p}$  is the coagulation rate of particles of diameter  $d_p$ , calculated by:

202

$$203 \quad \text{CoagS}_{d_p} = \int K(d_p, d'_p) n(d'_p) dd'_p \cong \sum_{d'_p=d_p}^{d'_p=\max} K(d_p, d'_p) N_{d_p}$$

204

205 as proposed by Kerminen et al. (2001).  $K(d_p, d'_p)$  is the coagulation coefficient of particle sizes  $d_p$   
206 and  $d'_p$ .  $S_{\text{losses}}$  accounts for the additional loss terms (i.e. chamber walls), not considered here. Initial  
207 particle formation starts at about  $1.5 \pm 0.4$  nm (Kulmala et al., 2012). The formation rate calculated  
208 here refers to particles in the atmosphere that reached the diameter of 10 nm during NPF events for  
209 uniformity reasons. This means that these particles were formed earlier during the day of the events,  
210 survived and grew to this size later in the day. Furthermore, due to the effect of the morning rush  
211 which biased the results at roadsides, the averages are calculated for the time window between 9:00  
212 to 15:00 ( $\pm 3$  hours from noon, when  $J_{10}$  peaked in the majority of the events). This was done for all  
213 the sites in this study for consistency.

214

215 As mentioned in the methodology for NPF event selection (chapter 2.2.1) days with particle  
216 formation resulting directly from traffic emissions were excluded. For those identified as NPF event  
217 days though, mainly for the roadside sites, formation associated with traffic emissions still occurs. It  
218 is impossible with the data available for this study to remove the traffic related particle formation in  
219 the calculations included in this study, by effectively separating it from secondary particle  
220 formation or calculate it. Using average conditions for comparison would lead to negative formation  
221 rate values in most cases, since in order for an NPF event to occur, traffic related particles are  
222 usually reduced to a greater extent compared to the formation from NPF, leading to lower particle  
223 concentrations on event days as found from a previous study in Marylebone Road, London  
224 (Bousiotis et al., 2019). This may result in an overestimation of the formation rates at roadside sites

225 presented in this study., The choice of a time window for which we would have the maximum effect  
226 of secondary particle formation and the minimum possible effect from traffic related particle  
227 formation attempts to reduce this discrepancy as much as possible.

228  
229 The Nucleation Strength Factor (NSF) proposed by Nemeth and Salma (2014) is a measure of the  
230 effect of NPF events on ultrafine particle concentration. It can either refer to the effect of NPF  
231 events on the day of their occurrence, calculated by:

$$232 \quad \text{NSF}_{\text{NUC}} = \frac{\left( \frac{N_{\text{smallest size available}-100\text{nm}}}{N_{100\text{nm}-\text{largest size available}}} \right)_{\text{nucleation days}}}{\left( \frac{N_{\text{smallest size available}-100\text{nm}}}{N_{100\text{nm}-\text{largest size available}}} \right)_{\text{non-nucleation days}}}$$

234  
235 or their overall contribution on the ultrafine particle concentrations at a site calculated by:

$$236 \quad \text{NSF}_{\text{GEN}} = \frac{\left( \frac{N_{\text{smallest size available}-100\text{nm}}}{N_{100\text{nm}-\text{largest size available}}} \right)_{\text{all days}}}{\left( \frac{N_{\text{smallest size available}-100\text{nm}}}{N_{100\text{nm}-\text{largest size available}}} \right)_{\text{non-nucleation days}}}$$

238  
239 The NPF event probability is a simple metric of the probability of NPF events calculated by the  
240 number of NPF event days divided by the number of days with available data for the given group

241 (temporal, wind direction etc.). Finally, it should be mentioned that all the results presented are  
242 normalised according the seasonal data availability for each site, based upon the expression:

$$243 \quad NPF_{probability} = \frac{N_{NPF \text{ event days for group of days } X}}{N_{days \text{ with available data for group of days } X}}$$

244

### 245 **3. RESULTS**

246 The seasonal NPF probability for all sites is found in Table S5. The annual number of NPF events,  
247 growth rate and formation rate for all the sites is found in Table S6, for which no clear interannual  
248 trend is found for any of the sites in this study. This may be due to the relatively short period of  
249 time studied for such variations to be observed.

250

#### 251 **3.1 Frequency and Seasonality of NPF Events**

252 In Denmark, NPF events occurred at all three sites with a similar frequency for the urban sites  
253 (5.4% for DENRO and 5.8% for DENUB) and higher for the rural DENRU site (7.9%). The  
254 seasonal variation favoured summer at DENRU and DENRO, while at DENUB a similar frequency  
255 for spring and summer was found (Figure 2). The within-week variation of the events favours  
256 weekends compared to weekdays going from the rural background site to the roadside site (Figure  
257 3). Interesting is the increased frequency of NPF events found in all Danish sites on Thursday  
258 among the weekdays. This trend though does not have a plausible explanation and is probably  
259 coincidental.

260

261 A higher frequency of events for all types of environments is found for the German sites compared  
262 to all other countries in this study. The background sites had NPF events for more than 17% of the  
263 days, while the roadside had a lower frequency of about 9%, with a seasonal variability favouring  
264 summer at all sites. It should be noted though that, due to the lack of spring and summer data for the  
265 first two years at the German roadside site, the frequency of events is probably a lot higher, and the  
266 seasonal variation should further favour these seasons. No substantial within-week variation was  
267 found for any of the sites in this country, a feature that is expected mainly at background sites. For  
268 GERRO, this may be due to not being as polluted as other sites of the same type, having an average  
269 condensation sink comparable to that of urban background sites in this study.

270

271 NPF events at the sites in Finland presented the most diverse seasonal variation, peaking at the  
272 background sites in spring and at the roadside site in summer (while the spring data availability is  
273 somewhat reduced for the Finnish roadside site, the general trend remains the same if all seasons  
274 had the same data availability). The frequency of NPF events at FINRU was higher (8.66%)  
275 compared to the urban sites (4.97% at FINUB and 5.20% at FINRO). Strong within-week variation  
276 favouring weekends is found for the roadside site, while no clear variation was found for the  
277 background sites. This may be due to either the higher condensation sink during weekdays that  
278 suppresses the events, or the dominant impact of the traffic emissions which could make the  
279 detection of NPF events harder.

280

281 For Spain, data was available for an urban and a rural background site in the greater area of  
282 Barcelona. NPF events were rather frequent, occurring on about 12% of the days at the rural  
283 background site and 13.1% at the urban site. Though the sites are in close proximity (about 50 km),  
284 the seasonality of NPF events was different between them, peaking in spring at SPARU and autumn  
285 at SPAUB. The frequency of NPF events in winter was relatively high compared to the sites in  
286 central and northern Europe and higher than summer for both sites. For both sites a higher NPF  
287 probability was found on weekends compared to weekdays, though this trend is stronger at SPAUB.  
288 Finally, for Greece data are available for two background sites, though not in close proximity (the  
289 distance between the sites is about 350 km). While in Greece meteorological conditions are  
290 favourable in general for NPF events, with high solar radiation and low relative humidity, their  
291 frequency was only 8.5% for the urban background site in Athens and 6.5% for the rural  
292 background site in Finokalia, similar to the frequency of Class I events reported in the study by  
293 Kalivitis et al. (2019). Most NPF events occurred in spring at both sites, peaking in April. It is  
294 interesting that the sites in southern Europe (in Spain and Greece) have a considerable number of  
295 NPF events during winter, which might be due to the specific meteorological conditions found in  
296 this area, where winter is a lot warmer than at the sites in northern and central Europe, and  
297 insolation is higher.

298

299

300



### 301 3.2 The Formation and Growth Rates

302 For the Danish sites the growth rate was found to be higher at the roadside site at  $4.45 \pm 1.87 \text{ nm h}^{-1}$   
303 and it was similar for the other two sites ( $3.19 \pm 1.43$  for DENRU and  $3.19 \pm 1.45$  for DENUB)  $\text{nm h}^{-1}$   
304 (Figure 4), though the peak was found in different seasons (Figure 5), coinciding with that of the  
305 frequency of NPF events (the highest average for DENRO was found for winter but it was only for  
306 a single event that occurred in that season). The formation rate ( $J_{10}$ ) was found to be broadly similar  
307 at the rural and urban background sites and higher at DENRO (Figure 6), favoured by different  
308 seasons at each site (summer at DENRU, spring at DENUB though with minimal differences and  
309 autumn at DENRO) (Figure 7).

310

311 Similar to the frequency of NPF events, the German sites also had higher growth rates compared to  
312 sites of the same type in other areas of this study, with GERRU having  $4.34 \pm 1.73 \text{ nm h}^{-1}$ , GERUB  
313  $4.24 \pm 1.69 \text{ nm h}^{-1}$  and GERRO  $5.17 \pm 2.20 \text{ nm h}^{-1}$  (Figure 3). While the difference between GERRU  
314 and GERUB is not statistically significant, there is a significant difference with GERRO ( $p <$   
315  $0.005$ ). Higher growth rates were found in summer compared to spring for all sites (Figure 5).  
316 Specifically, for the roadside though, the highest average growth rates were found in autumn, which  
317 may be either a site-specific feature or an artefact of the limited number of events in that season  
318 (total of 11 NPF events in autumn). Similarly,  $J_{10}$  at the German sites was also the highest among  
319 the sites of this study, increasing from the GERRU to GERRO. It was found to be higher in summer  
320 for the background sites and in autumn for GERRO.

321 For the Finnish sites, growth rates were similar at the background sites ( $2.91 \pm 1.68 \text{ nm h}^{-1}$  at FINRU  
322 and  $2.87 \pm 1.33 \text{ nm h}^{-1}$  at FINUB), peaking in the summer months, similar to the findings of Yli-Juuti  
323 et al. (2011), while the peak for FINRO (growth rate at  $3.74 \pm 1.48 \text{ nm h}^{-1}$ ) was found in spring,  
324 though the differences between the seasons for this site were rather small. The formation rate was  
325 the highest at FINRO, peaking in autumn for both urban sites (with small differences with spring),  
326 while FINRU presented the highest  $J_{10}$  in summer.

327

328 At the Spanish sites, the growth rate was similar for the two sites, being  $3.62 \pm 1.86 \text{ nm h}^{-1}$  at  
329 SPARU and  $3.38 \pm 1.53 \text{ nm h}^{-1}$  at SPAUB, again being higher in autumn for the urban site (which  
330 appears to be a feature of more polluted sites), while the rural site follows the general trend of rural  
331 background sites, peaking in summer. The formation rate at SPAUB is comparable to the other  
332 urban background sites (apart from GERUB) and peaked in spring, while once again the peak at  
333 SPARU was found in summer, similar to the other rural sites of this study apart from the Greek. At  
334 the urban site both the growth and formation rates were higher on weekdays compared to weekends  
335 (both  $p < 0.001$ ). While the higher growth rate during weekdays may be associated with the  
336 increased presence of condensable species from anthropogenic activities, the higher formation rate  
337 might be affected by the increased emissions during these days, which bias to an extent its value.  
338 Finally, the growth rate of particles was found to be similar at both Greek sites ( $3.68 \pm 1.41 \text{ nm h}^{-1}$   
339 for GREUB and  $3.78 \pm 2.01 \text{ nm h}^{-1}$  for GRERU) and was higher in summer compared to the other  
340 seasons, having a similar trend with the temperature and particulate organic carbon concentrations

341 in the area. The formation rate presented a unique trend, having high averages in winter for both  
342 sites. Interestingly, contrary to most background sites in this study, the lowest average  $J_{10}$  was found  
343 for summer at both sites.

344

### 345 **3.3 Conditions Affecting NPF Events**

346 The average and NPF event day conditions are presented in tables S2 and S3 (for meteorological  
347 conditions and atmospheric composition respectively). A number of variables present consistent  
348 behaviour on NPF days. For all the sites in this study the solar radiation intensity was higher on  
349 NPF days compared to the average conditions, while the relative humidity was lower. Additionally,  
350 all the chemical compounds with available data present either lower or similar concentrations. This  
351 is consistent even for the chemical compounds which are associated with the NPF process (such as  
352 the  $SO_2$ ). This probably indicates that they are in sufficient concentrations for not being a limiting  
353 factor in the occurrence of the events, while higher concentrations are associated with increased  
354 pollution conditions which may suppress their occurrence. The exceptions found are SPARU and  
355 GRERU for  $NO_2$  and FINRU for  $SO_2$ . In these sites the concentrations of these gaseous components  
356 are very low in general (being rural background sites) and were found to be only marginally higher  
357 on NPF event days. These differences indicate that the variability of these compounds is not playing  
358 a significant role in the occurrence of the events and thus should not be considered as an important  
359 factor. The ozone concentration though, was found to be consistently higher on event days  
360 compared to the average conditions at all sites regardless of their geographical location and type. As

361 the ozone concentration variability is directly associated with the solar radiation intensity, it is  
362 unknown whether it plays a direct role in the occurrence of the events or it is the result of its  
363 covariance with the solar radiation intensity.

364

365 Following that, differences were found in the variability of some of the meteorological conditions,  
366 as well as local conditions (either meteorological or specific pollution sources), which played a  
367 significant role in the occurrence and the metrics of NPF events across the sites of this study. These  
368 will be further explored in the following sections.

369

### 370 **3.3.1 Denmark**

371 The meteorological conditions that prevailed on NPF event days followed the general trend  
372 mentioned earlier, while wind speed and temperature were higher than average (consistently at all  
373 sites, meteorological condition variability was significant for all ( $p < 0.001$ ) except the wind speed).  
374 As meteorological data were available from the urban background site (the variation between the  
375 rural and urban sites should not be great since they are about 25 km away from each other), the  
376 average conditions for the three sites are almost the same, with the only variability being the data  
377 availability among the sites. Thus, the more common wind directions in the area are southwesterly;  
378 for all sites though the majority of NPF events are associated with direct westerly and northwesterly  
379 winds, similar to the findings of Wang et al. (2013) for the same site, which are those with the  
380 lowest concentrations of pollutants and condensation sink for all sites (Table S7), probably being of

381 marine origin as elemental concentrations showed an increased presence of Na, Cl and Mg (results  
382 not included). The wind directions with the highest probability for NPF events presented low  
383 growth rates and vice versa (Table S4), though it was proposed by Kristensson et al. (2008) that  
384 there is a possibility for events observed at the nearby Vavihill site in Sweden with northwesterly  
385 winds to be associated to the emissions of specific ship lanes that pass from that area. Wind  
386 direction sectors with higher concentrations of OC coincide with higher growth rates at DENRO,  
387 while this variability is not found at DENRU possibly showing that different compounds and  
388 mechanisms take part in the growth process of the newly formed particles (Kulmala et al., 2004b).  
389

390 As mentioned earlier, DENUB although close to the DENRO site has different seasonal variation of  
391 NPF events, with a marginally lower frequency in summer compared to the other two Danish sites,  
392 which have almost the same seasonal variation of NPF events. At DENUB, a strong presence of  
393 particles in the size range of about 50 – 60 nm is observed (Figure S1), especially during summer  
394 months, increasing the condensation sink in the area (this enhanced mode of particles is visible at  
395 DENRO as well, but its effect is dampened due to the elevated particle number concentrations in  
396 the other modes). This mode is probably part of the urban particle background. The strongest source  
397 though at DENUB appears to be from the east and consistently appears at both urban sites; this  
398 sector is where both elevated pollutant concentrations and condensation sink are found. In this  
399 sector, there are two possible local sources, either the port located 2 km to the east or the power  
400 plant located at a similar distance (or both). In general, both stations are located only a few

401 kilometres away from the Øresund strait, a major shipping route. Studying the SMPS plots it can be  
402 seen that NPF events at DENUB, especially in summer, tend to start but are either suppressed after  
403 the start or have a lifetime of a couple of hours before the new particles are scavenged or evaporate.  
404 While this might explain to an extent the frequency and variability of NPF events at this site, the  
405 balance between the condensation sink and the concentration of condensable compounds is  
406 highlighted. While at DENRO the condensation sink is considerably higher than at DENUB and the  
407 effect of the aforementioned mode of particles is present at both, the occurrence and development of  
408 NPF events at DENRO are more pronounced in the data, due to the higher concentrations of  
409 condensable compounds.

410

### 411 **3.3.2 Germany**

412 Compared to the average conditions, a higher temperature was found on NPF event days, while  
413 wind speed was lower at all German sites. The condensation sink was also higher on event days  
414 compared to the average, though this may be the result of the high formation rates found for the  
415 German sites. The wind profile is different between the urban and the rural sites, with mainly  
416 northeasterly and southwesterly winds at the rural site and a more balanced profile for the urban  
417 sites. This difference is probably due to differences in the local topography. For the urban sites the  
418 majority of NPF events are associated with easterly winds (to a lesser extent westerly as well for  
419 GERRO). At GERUB, along with the increased frequency of NPF events, the highest average  
420 growth rate is also found with easterly wind directions (though the differences are rather small). At

421 GERRO the frequency and growth rate appear to be affected by the topography of the site.  
422 Eisenbahnstraße is a road with an axis at almost  $90^{\circ} - 270^{\circ}$  and although the H/W ratio  
423 (surrounding building height to width ratio) is not high, the effect of a street canyon vortex is  
424 observed (Voigtländer et al., 2006). Possibly as a consequence of this, the probability of NPF events  
425 is low for direct northerly and southerly winds, although there are high growth rates of the newly  
426 formed particles (highest growth rates observed with southerly winds, associated with cleaner air).  
427  
428 At GERRU an increased probability of NPF events and growth rate are also found for wind  
429 directions from the easterly sector, although these are not very frequent for this site. For this site  
430 chemical composition data for  $PM_{2.5}$  and  $PM_{10}$  are available, and it is found that the generally low  
431 (on average) concentrations of pollutants (such as elemental carbon, nitrate and sulphate), in general  
432 are elevated for wind directions from that sector. This is also reported for the Melpitz site (GERRU)  
433 by Jaatinen et al. (2009) and probably indicates that in a relatively clean area, the presence of low  
434 concentrations of pollutants may be favourable in the occurrence and development of NPF events,  
435 as in general pollutant concentrations are lower on NPF event days compared to average conditions.  
436 Another interesting point is the concentration of organic carbon at the site (average of  $2.18 \mu\text{g m}^{-3}$   
437 in  $PM_{2.5}$ ), having the highest average concentration among the rural background sites studied. As  
438 other pollutant concentrations are relatively low at this site, it is possible that a portion of this  
439 organic carbon is of biogenic origin, considering also that the area is largely surrounded by forests  
440 and green areas, with a minimal effect of marine air masses (as indicated by the low marine

441 component concentrations – data not included) and possibly pointing to increased presence of  
442 BVOCs. The increased presence of organic species at GERRU may explain to some extent the  
443 increased frequency of NPF events as well as the highest growth and formation rates found among  
444 the sites of this study.

445

### 446 **3.3.3 Finland**

447 At the background sites in Finland, temperature was lower on NPF event days compared to the  
448 average conditions, whereas it was higher for FINRO associated with the different seasonality of  
449 the events. No significant differences were found for the wind speed on NPF events for all sites.  
450 There are though some significant differences in the wind conditions for NPF events compared to  
451 average conditions. At FINRU, NPF events were more common with northerly wind directions, as  
452 was also found by Nieminen et al. (2014) and Nilsson et al. (2001). This is probably due to the  
453 lower condensation sink which can be associated with the lower relative humidity also found for  
454 incoming winds from that sector and explains the lower temperatures found with NPF events at this  
455 site. Similarly, at FINUB NPF events were favoured by wind directions from the northerly sector,  
456 while there is almost a complete lack of NPF on southerly winds. This is due to its position at the  
457 north of both the city centre and the harbour, though winds from that sector are not common in  
458 general for that site. Finally, the wind profile for NPF events at FINRO also favours northerly winds  
459 with an almost complete absence of NPF in southerly winds, probably due to the elevated pollutant  
460 concentrations and condensation sink associated with them.



461 At all sites, NPF event days had a lower condensation sink compared to the average for the site. The  
462 seasonal variation of NPF events in Finland favouring spring, was explained by earlier work as the  
463 result of the seasonal variation of H<sub>2</sub>SO<sub>4</sub> concentrations (Nieminen et al., 2014), which in the area  
464 peak in spring. The variation of H<sub>2</sub>SO<sub>4</sub> concentrations is directly associated with SO<sub>2</sub> concentrations  
465 in the area, which follow a similar trend. The seasonal variation of NPF events at FINRO though  
466 cannot be explained by the variation of H<sub>2</sub>SO<sub>4</sub> in the area. SO<sub>2</sub> concentrations, which were available  
467 only for the nearby urban background site at Kalio (about 3 km away from FINRO) and may  
468 provide information upon the trends of SO<sub>2</sub> in the greater area, peak during January (probably due  
469 to increased heating in winter and the limited oxidation processes due to lower incoming solar  
470 radiation) and are higher during spring months compared to summer. In general, the variation of  
471 pollutant concentrations and the condensation sink is not great for the spring and summer seasons.  
472 The only variable out of the ones considered that may explain to an extent the seasonality of NPF  
473 events at the site is the increased concentrations of PM<sub>10</sub> found for spring months, which might be  
474 associated with road sanding and salting that takes place in Scandinavian countries during the  
475 colder months (Kupiainen et al., 2016) with emissions to the ambient air during spring months  
476 (Stojiljkovic et al., 2019). The source of these particles though is uncertain, as no major differences  
477 in the wind roses are found between the two seasons. Another study by Sarnela et al. (2015) at a  
478 different site in southern Finland attributed the seasonality of NPF events in Finland to the absence  
479 of H<sub>2</sub>SO<sub>4</sub> clusters during summer months due to a possible lack of stabilizing agents (e.g.  
480 ammonia). This could explain the limited number of small particles (smaller than 10 nm) at the

481 background sites during summer. In the more polluted environment at a roadside site these agents  
482 may exist, but such data was unfortunately not available.  
483  
484 Finally, a feature mentioned by Hao et al. (2018) in their study at the site of Hyytiälä, in which late  
485 particle growth is observed was also found in this study. This happened on about 20% of NPF days  
486 at FINRU (and a number of non-event days) and in most cases in early spring (before mid-April) or  
487 late autumn (after mid-September). New particles were formed and either did not grow or grew very  
488 slowly until later in the day when growth rates increased (Figure S2). In all these cases, growth  
489 started when solar radiation was very low or zero, which probably associates the growth of particles  
490 with nighttime chemistry leading to the formation of organonitrates (as found by the same study). A  
491 similar behaviour was also occasionally found at FINUB. Particle growth at late hours is not a  
492 unique feature for the Finnish sites, as it was found at all sites studied. What is different in the  
493 specific events is the lack or very slow growth during the daytime. Lower temperature ( $-0.81^{\circ}\text{C}$ ),  
494 incoming solar radiation ( $112 \text{ Wm}^{-2}$ ) and higher relative humidity (68.4%) occurred on event days  
495 with later growth, while no clear wind association was found. Lower concentrations of organic  
496 matter and nitrate were found throughout the days with later growth compared to the rest of the  
497 NPF days. The very high average particle number concentration in the smaller size bins is due to  
498 particles, though not growing to larger sizes for some time, persisting in the local atmosphere for  
499 hours. These results though should be used with caution due to the limited number of observations.  
500

#### 501 3.3.4 Spain

502 The atmospheric conditions favouring NPF events at both sites are similar to most other sites,  
503 though with lower wind speed on event days compared to the average conditions ( $p < 0.001$  at  
504 SPAUB). The wind profile between the two sites is different, with mainly northwesterly and  
505 southeasterly winds for SPARU (which seems to be affected by the local topography), while a more  
506 balanced profile is found at SPAUB. For both sites, though, increased probability for NPF events is  
507 found for westerly and northwesterly winds. These incoming wind directions originate from a rather  
508 clean area with low concentrations of pollutants and condensation sink. At SPARU, incoming wind  
509 from directions with higher concentrations of pollutants and condensation sink were associated with  
510 lower frequency of NPF events but higher growth rates. At SPAUB, NPF events were relatively  
511 rare and growth rates were lower with easterly wind directions, as air masses originating from that  
512 section have passed from the city centre and the industrial areas from the Besos River. Due to this,  
513 incoming air masses from these sectors had higher concentrations of pollutants and condensation  
514 sink.

515

516 While NPF events with subsequent growth of the particles were rare during summer, cases of bursts  
517 of particles in the smallest size range available were found to occur frequently, especially in August  
518 and July (the month with the fewest NPF events, despite the favourable meteorological conditions).  
519 In such cases, a new mode of particles appears in the smallest size available, persisting for many  
520 hours though without clear growth (brief or no growth is only observed), as reported by Dall'Osto

521 et al. (2012). Due to the lack of growth of the particles these burst events do not qualify as NPF  
522 events using the criteria set in the present study. These burst events are associated with southerly  
523 winds (known as Garbí-southwest and Migjorn-south in Catalan, which are common during the  
524 summer in the area) that bring a large number of particles smaller than 30 nm to the site from the  
525 nearby airport (located about 15 km to the southwest) and port (7 km south), as well as Saharan  
526 dust, increasing the concentrations of PM (Rodríguez et al., 2001) and thus suppressing NPF events  
527 due to the increased condensation sink.

528

529 Finally, the wind direction profile at SPARU appears to have a daily trend, with almost exclusively  
530 stronger southeasterly winds at about midday (Figure S3), probably due to a local mesoscale  
531 circulation caused by the increased solar activity during that time (which results in different heating  
532 patterns of the various land types in the greater area). These incoming southeast winds are more  
533 polluted and have a higher condensation sink (being affected by the city of Barcelona), and almost  
534 consistently bring larger particles at the site during the midday period. This may explain to an  
535 extent the lowest probability for NPF events from that sector, despite the very high concentrations  
536 of O<sub>3</sub> associated with them, with some extreme values well above 100 µg m<sup>-3</sup> (Querol et al., 2017).  
537 The highest average growth rates are also found from that direction.

538

539

540

### 541 3.3.5 Greece

542 Temperature and wind speed are found to be lower on NPF event days at the Greek sites, though the  
543 differences are minimal and are associated with the seasonal variability of the events. The wind rose  
544 in GREUB mainly consists of northeasterly and southwesterly winds. Due to its position, the site is  
545 heavily affected by emissions in Athens city centre with westerly winds, resulting in increased  
546 particle number concentrations and condensation sink. Despite this, the highest NPF probability and  
547 growth rates were found with a northwesterly wind directions. This may be due to them being  
548 associated with the highest solar radiation (probably the result of seasonal and diurnal variation),  
549 temperature and the lowest relative humidity, along with the highest condensation sink and particle  
550 number concentrations of almost all sizes. Chemical composition data was not available for  
551 GREUB, though SO<sub>2</sub> concentrations are rather low in Athens and kept declining after the economic  
552 crisis (Vrekoussis et al., 2013). The seasonality of SO<sub>2</sub> concentration in Athens favoured winter  
553 months and was at its lowest during summer for the period studied (YIIEKA, 2012) (this trend  
554 changed later as SO<sub>2</sub> concentrations further declined), which may also be a factor in the seasonality  
555 of NPF events, though this will be further discussed later.

556

557 At the GRERU site, the wind profile is mainly westerly, and though it coincides with the most  
558 important source of pollutants in the area, the city of Herakleio, its effect while observable is not  
559 significant due to the topography in the area. The wind profile for NPF events is similar to the  
560 average with significantly higher wind speeds ( $p < 0.001$ ). In general, GRERU has very low

561 pollutant concentrations, with an average NO of  $0.073 \mu\text{g m}^{-3}$ , NO<sub>2</sub> of  $0.52 \mu\text{g m}^{-3}$  and SO<sub>2</sub> in  
562 concentrations below 1 ppb (Kouvarakis et al., 2002). Due to this, the differences in the chemical  
563 composition in the atmosphere are also minimal. For the specific site two different patterns of  
564 development of NPF events were found. In one case, NPF events occurred in a rather clear  
565 background, while in the other one they were accompanied with an increase in number  
566 concentrations of larger particles or a new mode appearing at larger sizes (about a third of the  
567 events). No differences were found in the seasonal variation between the two groups; increased  
568 gaseous pollutant and particulate organic carbon concentrations were found for the second group  
569 (though the differences were rather small) and a wind rose that favoured southwesterly winds  
570 (originating from mainland Crete) instead of the northwesterly (originating from the sea) ones for  
571 the first group. The growth rate for the two groups was found to be  $3.56 \text{ nm h}^{-1}$  for the first group  
572 and  $4.17 \text{ nm h}^{-1}$  for the second, which might be due to the increased presence of condensable  
573 compounds. As the dataset starts from the particle size of 8.77 nm, the possibility that these  
574 particles were advected from nearby areas should not be overlooked, though they persisted and  
575 grew at the site. Other than that, no significant differences were found for the different wind  
576 directions.

577

578 As mentioned earlier, both sites had a very low frequency of events and J<sub>10</sub> in summer similar to  
579 previous studies also reporting few or no events during summer (Vratolis et al., 2019; Ždímal et al.,  
580 2011), though the incoming solar radiation is the highest and relative humidity is the lowest during

581 that season. This variation was also observed by Kalivitis et al. (2012) who associated the seasonal  
582 variation of NPF events at GRERU with the concentrations of atmospheric ions. The effect of the  
583 Etesian winds (known as Meltemia in Greek), which dominate the southern Aegean region during  
584 the summer months though should not be overlooked. These result in very strong winds with an  
585 average wind speed of  $8.15 \text{ m s}^{-1}$  during summer at the Finokalia site, and increased turbulence  
586 found in all years with available data, affecting both sites of this study. During this period,  $N_{<30\text{nm}}$   
587 drops to half or less compared to other seasons at both sites, while  $N_{>100\text{nm}}$  is at its maximum due to  
588 particle aging (Kalkavouras et al., 2017), increasing the condensation sink, especially in GRERU  
589 (the effect in GREUB is less visible due to both the wind profile, blowing from east which is a less  
590 polluted area, as well as the reduction of urban activities during summer months in Athens). Both  
591 the increased condensation sink and turbulence are possible factors for the reduced number of NPF  
592 events found at both sites in summer. Another possible factor is the effect of high temperatures in  
593 destabilising the molecular clusters critical to new particle formation.

594

### 595 **3.4 Region-Wide Events**

596 Region-wide events are NPF events which occur over large-scale areas, that may cover hundreds of  
597 kilometres (Shen et al., 2018). In the present study, NPF events that took place on the same day at  
598 both background sites (urban background and rural) are considered as regional and their conditions  
599 are studied (Table S8). The background sites in Greece were not considered due to the great  
600 distance between them (about 350 km). There is also uncertainty for the background sites in

601 Finland, where the distance is about 190 km, though a large number of days were found when NPF  
602 events occurred on the same day. The number of region-wide events per season (or the fraction of  
603 region-wide events to total NPF events) is found in Figure 8 and it appears as if they are more  
604 probable in spring at all the sites of the present study (apart from Finland, though the number of  
605 events in winter was low), despite the differences found in absolute numbers.

606 In Denmark, about 20% of NPF events in DENRU were regional (the percentage is higher for  
607 DENUB due to the smaller number of events, at 29%). The relatively low frequency of region-wide  
608 NPF events can be explained by the different seasonal dependence of NPF events (region-wide NPF  
609 events were more frequent in spring compared to the average due to the seasonality of NPF events  
610 in DENUB). Compared to local NPF event conditions, higher wind speed and solar radiation, as  
611 well as O<sub>3</sub> and marine compound concentrations (results not included) were found, while the  
612 concentrations of all pollutants (such as NO, NO<sub>x</sub>, sulphate, elemental and organic carbon) were  
613 lower. These cleaner atmospheric conditions are also confirmed by the lower CS associated with  
614 region-wide events, which is probably one of the most important factors in the occurrence of these  
615 large-scale events. The exceptions found at DENRU (increased relative humidity and less incoming  
616 solar radiation) are probably due to the different seasonality between local and region-wide NPF  
617 events at the site, though region-wide events rarely present similar characteristics at different sites  
618 even in the same country due to the differences in the initial meteorological and local conditions  
619 (Hussein et al., 2009). The growth rates of region-wide events were found to be lower than those of  
620 local events at both sites, which is probably associated with the limited concentrations of



621 condensable compounds due to the cleaner air masses of marine origin (as confirmed by the higher  
622 concentrations of marine compounds).

623

624 In Germany, the majority of NPF events of this study were region-wide (about 60%). Compared to  
625 the average, the meteorological conditions found for NPF event days compared to average  
626 conditions were more distinct for the region-wide events, with even lower wind speed and relative  
627 humidity and higher temperature and solar radiation, and all of these differences were significant ( $p$   
628  $< 0.001$ ). At GERRU where chemical composition data was available, higher concentrations of  
629 particulate organic carbon and sulphate and lower nitrate concentrations were found. The  
630 differences are significant ( $p < 0.001$ ) and may explain the higher growth rates found in region-wide  
631 events at both sites compared to the average, which is a unique feature. It should be noted that as  
632 the majority of NPF events at the German sites are associated with easterly winds, it is expected that  
633 in most cases the region-wide events will be associated with these, carrying the characteristics that  
634 come along with them (increased growth rates and concentrations of organic carbon, as discussed in  
635 Section 3.2).

636

637 In Finland, about a quarter of the NPF event days at FINRU (26%) occurred on the same day as at  
638 FINUB (the frequency is a lot higher for FINUB, at 39%). As in Germany, the meteorological  
639 conditions found on NPF event days compared to average conditions were more distinct during  
640 region-wide events. Thus, for both sites temperature and relative humidity were lower while solar

641 radiation was higher. The different trend found for the wind speed at the two sites (being higher on  
642 average NPF days at FINRU and lower at FINUB compared to average conditions) was enhanced  
643 as well at the two sites for region-wide events. At FINRU where chemical composition data was  
644 available, NO<sub>x</sub> and SO<sub>2</sub> had similar concentrations on region-wide event days compared to the  
645 averages on total event days, while O<sub>3</sub> was significantly higher ( $p < 0.001$ ). As at most other sites,  
646 the growth rate was found lower on region-wide event days compared to the average at both sites.  
647

648 Finally, in Spain the datasets of the two sites did not overlap greatly, having only 322 common  
649 days. Among these days, 13 days presented with NPF events that took place simultaneously at both  
650 sites, with smaller growth rates on average compared to local events (43% of the events at SPARU  
651 and 36% of the events at SPAUB in the period 8/2012 to 1/2013 and 2014 when data for both sites  
652 were available). Due to the small number of common events the results are quite mixed with the  
653 only consistent result being the lower relative humidity and higher O<sub>3</sub> concentrations for regional  
654 events at both sites, though none of these differences is significant. The wind profile at SPAUB  
655 seems to further favour the cleaner sector, with the majority of incoming winds being from the NW  
656 and even higher wind speeds (though with low significance). The result is similar at SPARU,  
657 though less clear and with lower wind speeds.

658  
659 These results are in general in agreement with those found in the UK in a previous study, where  
660 meteorological conditions were more distinct on region-wide event days compared to local NPF

661 events; pollutant concentrations were lower as well as the growth rates of the newly formed  
662 particles (Bousiotis et al., 2019).

663

664 Common events were also found between either of the background sites and the roadside, but they  
665 were always fewer in number, due to the difference in their temporal variability compared to the  
666 background sites, resulting from the effect of roadside pollution.

667

### 668 **3.5 The Effect of NPF Events on the Ultrafine Particle Concentrations**

669 The NSF is a metric of the effect of NPF events upon particle concentrations on either the days of  
670 the events or over a larger timescale. Both the  $NSF_{NUC}$  and  $NSF_{GEN}$  were calculated for all sites of  
671 this study and the results are presented in Figure 9. For almost all rural background sites  $NSF_{NUC}$ ,  
672 which indicates the effect of NPF on ultrafine particle concentrations on the day of the event, was  
673 found to be greater than 2 (the only exception was GERRU), which means that NPF events more  
674 than double the number of ultrafine particles (particles with diameter smaller than 100 nm) at the  
675 site on the days of the events, as NPF events are one of the main sources of ultrafine particles in this  
676 type of sites, especially below 30 nm. This reaches up to 4.18 found at FINRU (418% more  
677 ultrafine particles on the day of the events – 100% being the average), showing the great effect NPF  
678 events have on rather clean areas. The long-term effect was smaller, and it was found that at FINRU  
679 NPF events increase the number of ultrafine particles by an additional 130% in general. The effect  
680 of NPF events was a lot smaller at the urban sites, though still significant at urban background sites

681 (reaching up 240% at FINUB on the days of events), while roadsides had the smallest NSF  
682 compared to their respective background sites. This is because of the increased effect of local  
683 sources such as traffic or heating, and the associated increased condensation sink found within these  
684 sites, which cause the new particles to be scavenged by the more polluted background.

685

686 The calculation of NSF at the sites around Europe showed a weakness of the specific metric, which  
687 points to the need for more careful interpretation of the results of this metric, especially at roadside  
688 sites. At FINRO, the  $NSF_{NUC}$  provided a value smaller than 1, which translates as ultrafine particles  
689 are lost instead of formed on NPF event days. This though is the result of both the sharp reduction  
690 in particle number concentrations at all modes that are required for NPF events to occur at a busy  
691 roadside (much lower condensation sink), as well as a difference in the ratio between smaller to  
692 larger particles (smaller or larger than 100 nm) on NPF event days (favouring the larger particles) at  
693 the specific site. Similarly, the long-term effect of NPF events at the site was found to be 1, which  
694 means that NPF events appear to cause no changes in the number concentration of ultrafine  
695 particles.

696

## 697 **4. DISCUSSION**

### 698 **4.1 Variability of the Frequency and Seasonality of the Events**

699 A higher frequency of NPF events at the rural background sites compared to roadsides was found  
700 for all countries with available data for both types of site. This pattern comes in contrast with what

701 was found for the more polluted Asian cities (Peng et al., 2017; Wang et al., 2017), where NPF  
702 events were more frequent at the urban sites. This is probably associated with the even greater  
703 abundance of condensable species (which further enhances the growth of the particles, thus  
704 increasing their chance of survival), deriving from anthropogenic emissions, found in Asian  
705 megacities compared to European ones and results in a greater frequency of NPF events in Asian  
706 cities, even compared to the most polluted cities in Europe. This contrast emphasises the differences  
707 in the occurrence of NPF events between the polluted cities in Europe and Asia, which are  
708 associated with the level of pollution found in them, as well as the influence that the level of  
709 pollution has on the occurrence of NPF events in general.

710

711 The type of site dependence found in Europe together with the average conditions found on NPF  
712 event days compared to the average for each site, underline the importance of clear atmospheric  
713 conditions (high solar radiation and low relative humidity and pollutant concentrations) at all types  
714 of sites in Europe, especially for region-wide events. The temperature and wind speed presented  
715 more diverse results which in many cases are associated with local conditions. The origin of the  
716 incoming air masses though, appears to have a more important influence upon the NPF events.  
717 Cleaner air masses tend to have higher probability for NPF events, a result which was consistent  
718 among the sites of this study regardless of their type.

719

720 The frequency of NPF events at roadsides peaked in summer in all three countries with available  
721 data. Greater variability in the seasonality of NPF events was found at the background sites. The  
722 urban background sites presented more diverse results, for both the occurrence and development of  
723 NPF events, especially compared to rural background sites. The within-week variation of NPF  
724 events was found to favour weekends in most cases, as the pollution levels decrease, due to the  
725 weekly cycle, especially at the roadsides. As background sites have smaller variations between  
726 weekdays and weekends, the within-week variation of NPF events is smaller at the urban  
727 background sites and almost non-existent at the rural background sites. Finally, it should be noted  
728 that no clear interannual trend was found in the frequency of the events for any site, even for those  
729 with longer datasets.

730

#### 731 **4.2 Variability and Seasonality of the Formation and Growth Rate**

732 The growth rate of the newly formed particles was found to be higher at all the roadsides compared  
733 to their respective rural and urban background. The picture is similar for  $J_{10}$ , (the rate of formed  
734 particles associated with NPF events that reached 10 nm diameter), for which urban background  
735 sites were between their respective rural background sites and the roadsides with the sole exception  
736 of DENUB (the difference with DENRU is rather small though). The growth and formation rate at  
737 the rural background sites (apart from the Greek site) were found to be higher in summer compared  
738 to the other seasons. On the other hand, the seasonality of the growth rate at the roadsides is not  
739 clear but the formation rate peaks in the autumn at all three roadside sites. While the trend at the

740 rural sites is probably associated with the enhanced photochemistry and increased concentrations of  
741 BVOCs during summer, the seasonality of the growth rate at the roadside sites is more difficult to  
742 explain and probably shows the smaller importance of the BVOCs compared to the compounds of  
743 anthropogenic origin (which are in less abundance in summer) in this type of environment. In  
744 general, higher temperatures were associated with higher growth rates. This though applies only for  
745 the specific conditions at each site and cannot be used as a general rule for the expected growth rate  
746 at a site, as locations with higher temperatures did not present higher growth rates. Additionally, the  
747 origin of the incoming air masses appears to have an effect on the growth of the particles as well. In  
748 most of the sites in this study, incoming air masses from directions associated with higher  
749 concentrations of pollutants presented higher growth rates of the newly formed particles. The effect  
750 of the different wind directions upon the formation rate was more complex and a definitive  
751 conclusion cannot be made. Finally, as with the frequency of the events, no significant interannual  
752 trend was found in the variation of the formation or the growth rate across the sites studied.

753

#### 754 **4.3 Effect of Local Conditions in the Occurrence and Development of NPF Events**

755 Apart from the general meteorological and atmospheric conditions that affect the occurrence and  
756 the metrics of NPF events, conditions with a more local character were found to play a significant  
757 role as well. These include synoptic systems, such as the one occurring during the summer at the  
758 Greek sites, affecting the frequency and seasonality of the events. As a result, sites or seasons with  
759 conditions that favoured NPF presented decreased frequency of events and unexpected seasonality,

760 due to the increased turbulence caused by such pressure systems. Additionally, local sources of  
761 pollution can also have a significant impact in the temporal trends and metrics of the events, even  
762 for sites of very close proximity. One such example was the urban sites in Denmark, which despite  
763 being affected by the same source of pollution (the nearby port) and being only a few kilometres  
764 away from each other, presented different outcomes in the occurrence of the events. This was due to  
765 the different atmospheric composition found between them, being a background and a roadside site,  
766 which led to a different response in that local variable. In this case, the effect of the specific source  
767 was more prominent at the urban background site compared to the roadside, resulting in fewer NPF  
768 events, as the newly formed particles were more effectively suppressed at the urban background site,  
769 due to their slower growth.

770

## 771 **5. CONCLUSIONS**

772 There are different ways to assess the occurrence of new particle formation (NPF) events. In this  
773 study, the frequency of NPF events, the formation and growth rate of the particles associated with  
774 secondary formation of particles and not primary emissions, at 13 sites from five countries in  
775 Europe are considered. NPF is a complicated process, affected by many meteorological and  
776 environmental variables. The seasonality of these variables, which varies throughout Europe, results  
777 in the different temporal trends found for the metrics studied in this paper. Apart from  
778 meteorological conditions though, some of which have a uniform effect (such as the solar radiation  
779 intensity and relative humidity), many local variables can also have a positive or negative effect in



780 the occurrence of these events. Sites with less anthropogenic influence seem to have temporal  
781 trends dependant on the seasonality of synoptic conditions and general atmospheric composition.  
782 The urban sites though and especially those with significant sources of pollution in close proximity,  
783 present more complex trends as the NPF occurrence depends less upon favourable meteorological  
784 conditions and more upon the local atmospheric conditions, including composition. As NPF event  
785 occurrence is based on the balance between the rapid growth of the newly formed particles and their  
786 loss from processes, such as the evaporation or coagulation of the particles, the importance of  
787 significant particle formation, fast growth (which is enhanced by the increased presence of  
788 condensable compounds from anthropogenic activities found in urban environments) and low  
789 condensation sink is increased within such environments, also affecting the temporal trends of the  
790 events, making them more probable during periods with smaller pollution loads (e.g. summer,  
791 weekends). This explains the smaller frequency of NPF events at roadside sites compared to their  
792 respective background sites, despite the greater formation and growth rates observed in them.  
793 Consequently, NPF events have a smaller influence on the ultrafine particle load at the urban sites  
794 compared to background sites, due to both the increased presence of ultrafine particles from  
795 anthropogenic emissions as well as the smaller probability of ultrafine particles to survive in such  
796 environments.

797  
798 Nevertheless, NPF events are an important source of ultrafine particles in the atmosphere for all  
799 types of environment and are an important factor in the air quality of a given area. The present

800 study underlines the importance of both the synoptic and local conditions on NPF events, the mix of  
801 which not only affects their development but can also influence their occurrence even in areas of  
802 very close proximity. NPF is a complex process, affected by numerous variables, making it  
803 extremely difficult to predict any of its metrics without considering multiple factors. Since the  
804 mechanisms and general trends in NPF events are yet to be fully explained and understood, more  
805 laboratory and field studies are needed to generate greater clarity and predictive capability.

806

#### 807 **DATA ACCESSIBILITY**

808 Data supporting this publication are openly available from the UBIRA eData repository at  
809 <https://doi.org/10.25500/edata.bham.00000467>

810

#### 811 **AUTHOR CONTRIBUTIONS**

812 The study was conceived and planned by MDO and RMH who also contributed to the final  
813 manuscript. The data analysis was carried out by DB who also prepared the first draft of the  
814 manuscript. AM, JKN, CN, JVN, HP, NP, AA, GK, SV and KE have provided with the data for the  
815 analysis. FDP, XQ, DCB and TP provided advice on the analysis.

816

#### 817 **COMPETING INTERESTS**

818 The authors have no conflict of interests.

819

820 **ACKNOWLEDGMENTS**

821 This work was supported by the National Centre for Atmospheric Science funded by the U.K.

822 Natural Environment Research Council (R8/H12/83/011).

823 **REFERENCES**

824

825 Aalto, P., Hämeri, K., Becker, E. D. O., Weber, R., Salm, J., Mäkelä, J. M., Hoell, C., O'Dowd, C.  
826 D., Karlsson, H., Hansson, H., Väkevä, M., Koponen, I. K., Buzorius, G. and Kulmala, M.: Physical  
827 characterization of aerosol particles during nucleation events, *Tellus, Ser. B Chem. Phys. Meteorol.*,  
828 53(4), 344–358, doi:10.3402/tellusb.v53i4.17127, 2001.

829

830 Alam, A., Shi, J. P. and Harrison, R. M.: Observations of new particle formation in urban air, *J.*  
831 *Geophys. Res. Atmos.*, 108(D3), 4093, doi:10.1029/2001JD001417, 2003.

832

833 Atkinson, R. W., Fuller, G. W., Anderson, H. R., Harrison, R. M. and Armstrong, B.: Urban  
834 ambient particle metrics and health: A time-series analysis, *Epidemiology*, 21(4), 501–511,  
835 doi:10.1097/EDE.0b013e3181debc88, 2010.

836

837 Bianchi, F., Kurtén, T., Riva, M., Mohr, C., Rissanen, M. P., Roldin, P., Berndt, T., Crouse, J. D.,  
838 Wennberg, P. O., Mentel, T. F., Wildt, J., Junninen, H., Jokinen, T., Kulmala, M., Worsnop, D. R.,  
839 Thornton, J. A., Donahue, N., Kjaergaard, H. G. and Ehn, M.: Highly oxygenated organic  
840 molecules (HOM) from gas-phase autoxidation involving peroxy radicals : A key contributor to  
841 atmospheric aerosol, *Chem. Rev.*, 119, 3472–3509, doi:10.1021/acs.chemrev.8b00395, 2019.

842

843 Birmili, W., Weinhold, K., Rasch, F., Sonntag, A., Sun, J., Merkel, M., Wiedensohler, A., Bastian,  
844 S., Schladitz, A., Löschau, G., Cyrus, J., Pitz, M., Gu, J., Kusch, T., Flentje, H., Quass, U.,  
845 Kaminski, H., Kuhlbusch, T. A. J., Meinhardt, F., Schwerin, A., Bath, O., Ries, L., Wirtz, K. and  
846 Fiebig, M.: Long-term observations of tropospheric particle number size distributions and  
847 equivalent black carbon mass concentrations in the German Ultrafine Aerosol Network (GUAN),  
848 *Earth Syst. Sci. Data*, 8(2), 355–382, doi:10.5194/essd-8-355-2016, 2016.

849

850 Bousiotis, D., Osto, M. D., Beddows, D. C. S., Pope, F. D., Harrison, R. M. and Harrison, C. R. M.:  
851 Analysis of new particle formation ( NPF ) events at nearby rural , urban background and urban  
852 roadside sites, 19, 5679–5694, 2019.

853

854 Boy, M., Kulmala, M., Ruuskanen, T. M., Pihlatie, M., Reissell, A., Aalto, P. P., Keronen, P., Dal  
855 Maso, M., Hellen, H., Hakola, H., Jansson, R., Hanke, M. and Arnold, F.: Sulphuric acid closure  
856 and contribution to nucleation mode particle growth, *Atmos. Chem. Phys.*, 5(4), 863–878,  
857 doi:10.5194/acp-5-863-2005, 2005.

858

859 Brean, J., Harrison, R. M., Shi, Z., Beddows, D. C. S., Acton, W. J. F. and Hewitt, C. N.:  
860 Observations of highly oxidised molecules and particle nucleation in the atmosphere of Beijing,  
861 *Atmos. Chem. Phys.*, 19, 14933–14947, 2019, doi.org/10.5194/acp-19-14933-2019, 2019.

862

863 Brines, M., Dall'Osto, M., Beddows, D. C. S., Harrison, R. M., Gómez-Moreno, F., Núñez, L.,  
864 Artíñano, B., Costabile, F., Gobbi, G. P., Salimi, F., Morawska, L., Sioutas, C. and Querol, X.:  
865 Traffic and nucleation events as main sources of ultrafine particles in high-insolation developed  
866 world cities, *Atmos. Chem. Phys.*, 15(10), 5929–5945, doi:10.5194/acp-15-5929-2015, 2015.  
867

868 Brines, M., Dall'Osto, M., Beddows, D. C. S., Harrison, R. M. and Querol, X.: Simplifying aerosol  
869 size distributions modes simultaneously detected at four monitoring sites during SAPUSS, *Atmos.*  
870 *Chem. Phys.*, 14(6), 2973–2986, doi:10.5194/acp-14-2973-2014, 2014.  
871

872 Carnerero, C., Pérez, N., Reche, C., Ealo, M., Titos, G., Lee, H., Eun, R., Park, Y., Dada, L.,  
873 Paasonen, P., Kerminen, V., Mantilla, E., Escudero, M., Gómez-moreno, F. J., Alonso-blanco, E.,  
874 Coz, E., Saiz-, A., Temime-roussel, B., Marchand, N., Beddows, D. C. S. and Harrison, R. M.:  
875 Vertical and horizontal distribution of regional new particle formation events in Madrid, *Atmos.*  
876 *Chem. Phys.*, 1–27, doi:10.5194/acp-2018-173, 2018.  
877

878 Charron, A., Birmili, W. and Harrison, R. M.: Fingerprinting particle origins according to their size  
879 distribution at a UK rural site, *J. Geophys. Res. Atmos.*, 113(7), 1–15, doi:10.1029/2007JD008562,  
880 2008.  
881

882 Cheung, H. C., Chou, C. C.-K., Huang, W.-R. and Tsai, C.-Y.: Characterization of ultrafine particle  
883 number concentration and new particle formation in an urban environment of Taipei, Taiwan,  
884 *Atmos. Chem. Phys.*, 13(17), 8935–8946, doi:10.5194/acp-13-8935-2013, 2013.  
885

886 Chu, B., Kerminen, V., Bianchi, F., Yan, C., Petäjä, T. and Kulmala, M.: Atmospheric new particle  
887 formation in China, *Atmos. Chem. Phys.*, 19, 115–138, doi.org/10.5194/acp-19-115-2019, 2019.  
888

889 Costabile, F., Birmili, W., Klose, S., Tuch, T., Wehner, B., Wiedensohler, A., Franck, U., König, K.  
890 and Sonntag, A.: Spatio-temporal variability and principal components of the particle number size  
891 distribution in an urban atmosphere, *Atmos. Chem. Phys.*, 9(9), 3163–3195, doi:10.5194/acp-9-  
892 3163-2009, 2009.  
893

894 Dal Maso, M., Kulmala, M., Riipinen, I., Wagner, R., Hussein, T., Aalto, P. P. and Lehtinen, K. E.  
895 J.: Formation and growth of fresh atmospheric aerosols: Eight years of aerosol size distribution data  
896 from SMEAR II, Hyytiälä, Finland, *Boreal Environ. Res.*, 10(5), 323–336,  
897 doi:10.1016/j.ijpharm.2012.03.044, 2005.  
898

899 Dal Maso, M., Kulmala, M., Lehtinen, K. E. J., Mäkelä, J. M., Aalto, P. and O'Dowd, C. D.:  
900 Condensation and coagulation sinks and formation of nucleation mode particles in coastal and  
901 boreal forest boundary layers, *J. Geophys. Res. Atmos.*, 107(19), doi:10.1029/2001JD001053, 2002.  
902

903 Dall'Osto, M., Beddows, D. C. S., Asmi, A., Poulain, L., Hao, L., Freney, E., Allan, J. D.,  
904 Canagaratna, M., Crippa, M., Bianchi, F., De Leeuw, G., Eriksson, A., Swietlicki, E., Hansson, H.  
905 C., Henzing, J. S., Granier, C., Zemankova, K., Laj, P., Onasch, T., Prevot, A., Putaud, J. P.,  
906 Sellegri, K., Vidal, M., Virtanen, A., Simo, R., Worsnop, D., O'Dowd, C., Kulmala, M. and  
907 Harrison, R. M.: Novel insights on new particle formation derived from a pan-european observing  
908 system, *Sci. Rep.*, 8(1), 1–11, doi:10.1038/s41598-017-17343-9, 2018.

909  
910 Dall'Osto, M., Querol, X., Alastuey, A., O'Dowd, C., Harrison, R. M., Wenger, J. and Gómez-  
911 Moreno, F. J.: On the spatial distribution and evolution of ultrafine particles in Barcelona, *Atmos.*  
912 *Chem. Phys.*, 13(2), 741–759, doi:10.5194/acp-13-741-2013, 2013.

913  
914 Dall'Osto, M., Beddows, D. C. S., Pey, J., Rodriguez, S., Alastuey, A., M. Harrison, R. and Querol,  
915 X.: Urban aerosol size distributions over the Mediterranean city of Barcelona, NE Spain, *Atmos.*  
916 *Chem. Phys.*, 12(22), 10693–10707, doi:10.5194/acp-12-10693-2012, 2012.

917  
918 Dameto de España, C., Wonaschütz, A., Steiner, G., Rosati, B., Demattio, A., Schuh, H. and  
919 Hitznerberger, R.: Long-term quantitative field study of New Particle Formation (NPF) events as a  
920 source of Cloud Condensation Nuclei (CCN) in the urban background of Vienna, *Atmos. Environ.*,  
921 164, 289–298, doi:10.1016/j.atmosenv.2017.06.001, 2017.

922  
923 Deng C., Fu, F., Dada, L., Yan, C., Cai, R., Yang, D., Zhou, Y., Yin, R., Lu, Y., Li, X., Fan, X.,  
924 Nie, W., Kontkanen, J., Kangasluoma, J., Chu, B., Ding, A., Kerminen, V.-M., Paasonen, P.,  
925 Worsnop, D.R., Bianchi, F., Liu, Y., Zheng, J., Wang, L., Kulmala, M. and Jiang, J.: Seasonal  
926 Characteristics of New Particle Formation and Growth in Urban Beijing, *Environ. Sci. Technol.*, 54,  
927 8547 – 8557, 2020.

928  
929 Ehn, M., Thornton, J. A., Kleist, E., Sipilä, M., Junninen, H., Pullinen, I., Springer, M., Rubach, F.,  
930 Tillmann, R., Lee, B., Lopez-Hilfiker, F., Andres, S., Acir, I. H., Rissanen, M., Jokinen, T.,  
931 Schobesberger, S., Kangasluoma, J., Kontkanen, J., Nieminen, T., Kurtén, T., Nielsen, L. B.,  
932 Jørgensen, S., Kjaergaard, H. G., Canagaratna, M., Maso, M. D., Berndt, T., Petäjä, T., Wahner, A.,  
933 Kerminen, V. M., Kulmala, M., Worsnop, D. R., Wildt, J. and Mentel, T. F.: A large source of low-  
934 volatility secondary organic aerosol, *Nature*, 506(7489), 476–479, doi:10.1038/nature13032, 2014.

935  
936 Fuchs, N. A. and Sutugin, A. G.: Highly dispersed aerosols, *Foreign Sci. Technol. Center*, 1-86,  
937 1971.

938  
939 Hama, S. M. L., Cordell, R. L., Kos, G. P. A., Weijers, E. P. and Monks, P. S.: Sub-micron particle  
940 number size distribution characteristics at two urban locations in Leicester, *Atmos. Res.*, 194, 1–16,  
941 doi:10.1016/j.atmosres.2017.04.021, 2017.

942

943 Hao, L., Garmash, O., Ehn, M., Miettinen, P., Massoli, P., Mikkonen, S. and Jokinen, T.: Combined  
944 effects of boundary layer dynamics and atmospheric chemistry on aerosol composition during new  
945 particle formation periods, *Atmos. Chem. Phys.*, 18, 17705–17716, doi.org/10.5194/acp-18-17705-  
946 2018, 2018.

947

948 Harrison, R. M., Shi, J. P., Xi, S., Khan, A., Mark, D., Kinnersley, R. and Yin, J.: Measurement of  
949 number, mass and size distribution of particles in the atmosphere, *Philos. Trans. R. Soc. A Math.*  
950 *Phys. Eng. Sci.*, 358(1775), 2567–2580, doi:10.1098/rsta.2000.0669, 2000.

951

952 Hietikko, R., Kuuluvainen, H., Harrison, R. M., Portin, H., Timonen, H., Niemi, J. V and Rönkkö,  
953 T.: Diurnal variation of nanocluster aerosol concentrations and emission factors in a street canyon,  
954 *Atmos. Environ.*, 189, 98–106, doi:10.1016/j.atmosenv.2018.06.031, 2018.

955

956 Hofman, J., Staelens, J., Cordell, R., Stroobants, C., Zikova, N., Hama, S. M. L., Wyche, K. P.,  
957 Kos, G. P. A., Van Der Zee, S., Smallbone, K. L., Weijers, E. P., Monks, P. S. and Roekens, E.:  
958 Ultrafine particles in four European urban environments: Results from a new continuous long-term  
959 monitoring network, *Atmos. Environ.*, 136, 68–81, doi:10.1016/j.atmosenv.2016.04.010, 2016.

960

961 Hussein, T., Junninen, H., Tunved, P., Kristensson, A., Dal Maso, M., Riipinen, I., Aalto, P. P.,  
962 Hansson, H. C., Swietlicki, E. and Kulmala, M.: Time span and spatial scale of regional new  
963 particle formation events over Finland and Southern Sweden, *Atmos. Chem. Phys.*, 9(14), 4699–  
964 4716, doi:10.5194/acp-9-4699-2009, 2009.

965

966 Iida, K., Stolzenburg, M. R., McMurry, P. H. and Smith, J. N.: Estimating nanoparticle growth rates  
967 from size-dependent charged fractions: Analysis of new particle formation events in Mexico City, *J.*  
968 *Geophys. Res. Atmos.*, 113(5), 1–15, doi:10.1029/2007JD009260, 2008.

969

970 Jaatinen, A., Hamed, A., Joutsensaari, J., Mikkonen, S., Birmili, W., Wehner, B., Spindler, G.,  
971 Wiedensohler, A., Decesari, S., Mircea, M., Facchini, M. C., Junninen, H., Kulmala, M., Lehtinen,  
972 K. E. J. and Laaksonen, A.: A comparison of new particle formation events in the boundary layer at  
973 three different sites in Europe, *Boreal Environ. Res.*, 14(4), 481–498, 2009.

974

975 Järvi, L., Hannuniemi, H., Hussein, T., Junninen, H., Aalto, P., Hillamo, R., Mäkelä, T., Keronen,  
976 P. and Siivola, E.: The urban measurement station SMEAR III : Continuous monitoring of air  
977 pollution and surface – atmosphere interactions in Helsinki , Finland, *Boreal Environ. Res.*, 14(4),  
978 86–109, 2009.

979

980 Jeong, C.-H. H., Evans, G. J., McGuire, M. L., Y.-W. Chang, R., Abbatt, J. P. D. D., Zeromskiene,  
981 K., Mozurkewich, M., Li, S.-M. M., Leitch, W. R., Chang, R. Y.-W., Abbatt, J. P. D. D.,  
982 Zeromskiene, K., Mozurkewich, M., Li, S.-M. M. and Leitch, W. R.: Particle formation and

983 growth at five rural and urban sites, *Atmos. Chem. Phys.*, 10(16), 7979–7995, doi:10.5194/acp-10-  
984 7979-2010, 2010.

985

986 Kalivitis, N., Stavroulas, I., Bougiatioti, A., Kouvarakis, G., Gagné, S., Manninen, H. E., Kulmala,  
987 M. and Mihalopoulos, N.: Night-time enhanced atmospheric ion concentrations in the marine  
988 boundary layer, *Atmos. Chem. Phys.*, 12(8), 3627–3638, doi:10.5194/acp-12-3627-2012, 2012.

989

990 Kalivitis, N., Kerminen, V.-M., Kulmala, M., Kanakidou, M., Myriokefalitakis, S., Tzitzikalaki, E.,  
991 Roldin, P., Kouvarakis, G., Stavroulas, I., Boy, M., Manninen, H. E., Bougiatioti, A., Daskalakis,  
992 N., Petäjä, T., Kalkavouras, P. and Mihalopoulos, N.: Formation and growth of atmospheric  
993 nanoparticles in the eastern Mediterranean: Results from long-term measurements and process  
994 simulations, *Atmos. Chem. Phys.*, 19, 2671–2686, doi.org/10.5194/acp-19-2671-2019, 2019.

995

996 Kalivitis, N., Kerminen, V. M., Kouvarakis, G., Stavroulas, I., Bougiatioti, A., Nenes, A.,  
997 Manninen, H. E., Petäjä, T., Kulmala, M. and Mihalopoulos, N.: Atmospheric new particle  
998 formation as a source of CCN in the eastern Mediterranean marine boundary layer, *Atmos. Chem.*  
999 *Phys.*, 15(16), 9203–9215, doi:10.5194/acp-15-9203-2015, 2015.

1000

1001 Kalkavouras, P., Bossioli, E., Bezantakos, S., Bougiatioti, A., Kalivitis, N., Stavroulas, I.,  
1002 Kouvarakis, G., Protonotariou, A. P., Dandou, A., Biskos, G., Mihalopoulos, N., Nenes, A. and  
1003 Tombrou, M.: New particle formation in the southern Aegean Sea during the Etesians: Importance  
1004 for CCN production and cloud droplet number, *Atmos. Chem. Phys.*, 17(1), 175–192,  
1005 doi:10.5194/acp-17-175-2017, 2017.

1006

1007 Kerminen, V.-M., Chen, X., Vakkari, V., Petäjä, T., Kulmala, M. and Bianchi, F.: Atmospheric new  
1008 particle formation and growth: review of field observations, *Environ. Res. Lett.*, 13(10), 103003,  
1009 doi:10.1088/1748-9326/aadf3c, 2018.

1010

1011 Kerminen, V. M., Lehtinen, K. E. J., Anttila, T. and Kulmala, M.: Dynamics of atmospheric  
1012 nucleation mode particles: A timescale analysis, *Tellus, Ser. B Chem. Phys. Meteorol.*, 56(2), 135–  
1013 146, doi:10.3402/tellusb.v56i2.16411, 2004.

1014

1015 Kerminen, V. M., Pirjola, L. and Kulmala, M.: How significantly does coagulation scavenging  
1016 limit atmospheric particle production?, *J. Geophys. Res. Atmos.*, 106(D20), 24119–24125,  
1017 doi:10.1029/2001JD000322, 2001.

1018

1019 Ketzel, M., Wählin, P., Kristensson, A., Swietlicki, E., Berkowicz, R., Nielsen, O. J. and Palmgren,  
1020 F.: Particle size distribution and particle mass measurements at urban, near-city and rural level in  
1021 the Copenhagen area and Southern Sweden, *Atmos. Chem. Phys.*, 4(1), 5513–5546,  
1022 doi:10.5194/acpd-3-5513-2003, 2004.



1023 Korhonen, P., Kulmala, M., Laaksonen, A., Viisanen, Y., Mcgraw, R. and Seinfeld, J. H.: Ternary  
1024 nucleation of H<sub>2</sub>SO<sub>4</sub>, NH<sub>3</sub> and H<sub>2</sub>O in the atmosphere, *J. Geophys. Res.*, 104(D21), 26349–26353,  
1025 doi.org/10.1029/1999JD900784, 1999.  
1026

1027 Kouvarakis, G., Bardouki, H. and Mihalopoulos, N.: Sulfur budget above the Eastern  
1028 Mediterranean: Relative contribution of anthropogenic and biogenic sources, *Tellus, Ser. B Chem.*  
1029 *Phys. Meteorol.*, 54(3), 201–212, doi:10.3402/tellusb.v54i3.16661, 2002.  
1030

1031 Kristensson, A., Dal Maso, M., Swietlicki, E., Hussein, T., Zhou, J., Kerminen, V. M. and Kulmala,  
1032 M.: Characterization of new particle formation events at a background site in southern Sweden:  
1033 Relation to air mass history, *Tellus, Ser. B Chem. Phys. Meteorol.*, 60 B(3), 330–344, 2008.  
1034

1035 Kulmala, M., Kontkanen, J., Junninen, H., Lehtipalo, K., Manninen, H. E., Nieminen, T., Petäjä, T.,  
1036 Sipilä, M., Schobesberger, S., Rantala, P., Franchin, A., Jokinen, T., Järvinen, E., Äijälä, M.,  
1037 Kangasluoma, J., Hakala, J., Aalto, P. P., Paasonen, P., Mikkilä, J., Vanhanen, J., Aalto, J., Hakola,  
1038 H., Makkonen, U., Ruuskanen, T., Mauldin, R. L., Duplissy, J., Vehkamäki, H., Bäck, J., Kulmala,  
1039 M., Petäjä, T., Ehn, M., Thornton, J., Sipilä, M., Worsnop, D. R. and Kerminen, V.-M.: Chemistry  
1040 of atmospheric nucleation: On the recent advances on precursor characterization and atmospheric  
1041 cluster composition in connection with atmospheric new particle formation, *Annu. Rev. Phys.*  
1042 *Chem.*, 65(1), 21–37, doi:10.1146/annurev-physchem-040412-110014, 2014.  
1043

1044 Kortelainen, A., Riipinen, I., Kurtén, T., Johnston, M. V., Smith, J. N., Ehn, M., Mentel, T. F.,  
1045 Lehtinen, K. E. J., Laaksonen, A., Kerminen, V. M. and Worsnop, D. R.: Direct observations of  
1046 atmospheric aerosol nucleation, *Science (80-. )*, 339(6122), 943–946,  
1047 doi:10.1126/science.1227385, 2013.  
1048

1049 Kulmala, M., Petäjä, T., Nieminen, T., Sipilä, M., Manninen, H. E., Lehtipalo, K., Dal Maso, M.,  
1050 Aalto, P. P., Junninen, H., Paasonen, P., Riipinen, I., Lehtinen, K. E. J., Laaksonen, A. and  
1051 Kerminen, V. M.: Measurement of the nucleation of atmospheric aerosol particles, *Nat. Protoc.*,  
1052 7(9), 1651–1667, doi:10.1038/nprot.2012.091, 2012.  
1053

1054 Kulmala, M., Petäjä, T., Mönkkönen, P., Koponen, I. K., Dal Maso, M., Aalto, P. P., Lehtinen, K.  
1055 E. J. and Kerminen, V.-M.: On the growth of nucleation mode particles: source rates of condensable  
1056 vapor in polluted and clean environments, *Atmos. Chem. Phys. Discuss.*, 4(5), 6943–6966,  
1057 doi:10.5194/acpd-4-6943-2004, 2005.  
1058

1059 Kulmala, M., Vehkamäki, H., Petäjä, T., Dal Maso, M., Lauri, A., Kerminen, V. M., Birmili, W.  
1060 and McMurry, P. H.: Formation and growth rates of ultrafine atmospheric particles: A review of  
1061 observations, *J. Aerosol Sci.*, 35(2), 143–176, doi:10.1016/j.jaerosci.2003.10.003, 2004a.  
1062

1063 Kulmala, M., Laakso, L., Lehtinen, K. E. J., Riipinen, I., Dal Maso, M., Anttila, T., Kerminen, V.-  
1064 M., Hörrak, U., Vana, M. and Tammet, H.: Initial steps of aerosol growth, *Atmos. Chem. Phys.*  
1065 *Discuss.*, 4(5), 5433–5454, doi:10.5194/acpd-4-5433-2004, 2004b.  
1066  
1067 Kulmala, M., Dal Maso, M., Mäkelä, J. M., Pirjola, L., Väkevä, M., Aalto, P., Miikkulainen, P.,  
1068 Hämeri, K. and O’Dowd, C. D.: On the formation, growth and composition of nucleation mode  
1069 particles, *Tellus, Ser. B Chem. Phys. Meteorol.*, 53(4), 479–490, doi:10.3402/tellusb.v53i4.16622,  
1070 2001.  
1071  
1072 Kumar, P., Morawska, L., Birmili, W., Paasonen, P., Hu, M., Kulmala, M., Harrison, R. M.,  
1073 Norford, L. and Britter, R.: Ultrafine particles in cities, *Environ. Int.*, 66, 1–10,  
1074 doi:10.1016/j.envint.2014.01.013, 2014.  
1075  
1076 Kupiainen, K., Ritola, R., Stojiljkovic, A., Pirjola, L., Malinen, A. and Niemi, J.: Contribution of  
1077 mineral dust sources to street side ambient and suspension PM<sub>10</sub> samples, *Atmos. Environ.*, 147,  
1078 178–189, doi:10.1016/j.atmosenv.2016.09.059, 2016.  
1079  
1080 Li, X., Chee, S., Hao, J., Abbatt, J. P. D., Jiang, J. and Smith, J. N.: Relative humidity effect on the  
1081 formation of highly oxidized molecules and new particles during monoterpene oxidation, *Atmos.*  
1082 *Chem. Phys.*, 19(3), 1555–1570, doi:10.5194/acp-19-1555-2019, 2019.  
1083  
1084 Ma, N. and Birmili, W.: Estimating the contribution of photochemical particle formation to ultrafine  
1085 particle number averages in an urban atmosphere, *Sci. Total Environ.*, 512–513, 154–166,  
1086 doi:10.1016/j.scitotenv.2015.01.009, 2015.  
1087  
1088 Makkonen, R., Asmi, A., Kerminen, V. M., Boy, M., Arneth, A., Hari, P. and Kulmala, M.: Air  
1089 pollution control and decreasing new particle formation lead to strong climate warming, *Atmos.*  
1090 *Chem. Phys.*, 12(3), 1515–1524, doi:10.5194/acp-12-1515-2012, 2012.  
1091  
1092 Masiol, M., Harrison, R. M., Vu, T. V. and Beddows, D. C. S.: Sources of sub-micrometre particles  
1093 near a major international airport, *Atmos. Chem. Phys.*, 17(20), 12379–12403, doi:10.5194/acp-17-  
1094 12379-2017, 2017.  
1095  
1096 McFiggans, G., Mentel, T. F., Wildt, J., Pullinen, I., Kang, S., Kleist, E., Schmitt, S., Springer, M.,  
1097 Tillmann, R., Wu, C., Zhao, D., Hallquist, M., Faxon, C., Le Breton, M., Hallquist, Å. M., Simpson,  
1098 D., Bergström, R., Jenkin, M. E., Ehn, M., Thornton, J. A., Alfarra, M. R., Bannan, T. J., Percival,  
1099 C. J., Priestley, M., Topping, D. and Kiendler-Scharr, A.: Secondary organic aerosol reduced by  
1100 mixture of atmospheric vapours, *Nature*, 565(7741), 587–593, doi:10.1038/s41586-018-0871-y,  
1101 2019.  
1102

1103 Minguillón, M. C., Brines, M., Pérez, N., Reche, C., Pandolfi, M., Fonseca, A. S., Amato, F.,  
1104 Alastuey, A., Lyasota, A., Codina, B., Lee, H. K., Eun, H. R., Ahn, K. H. and Querol, X.: New  
1105 particle formation at ground level and in the vertical column over the Barcelona area, *Atmos. Res.*,  
1106 164–165, 118–130, doi:10.1016/j.atmosres.2015.05.003, 2015.  
1107  
1108 Napari, I., Noppel, M., Vehkamäki, H. and Kulmala, M.: An improved model for ternary nucleation  
1109 of sulfuric acid-ammonia-water, *J. Chem. Phys.*, 116(10), 4221–4227, doi:10.1063/1.1450557,  
1110 2002.  
1111  
1112 Németh, Z. and Salma, I.: Spatial extension of nucleating air masses in the Carpathian Basin,  
1113 *Atmos. Chem. Phys.*, 14(16), 8841–8848, doi:10.5194/acp-14-8841-2014, 2014.  
1114  
1115 Nieminen, T., Asmi, A., Maso, M. D., Aalto, P. P., Keronen, P., Petäjä, T., Kulmala, M. and  
1116 Kerminen, V.: Trends in atmospheric new-particle formation : 16 years of observations in a boreal-  
1117 forest environment, *Boreal Environ. Res.*, 19, 191–214, 2014.  
1118  
1119 Nilsson, E. D., Rannik, Ü., Kulmala, M., Buzorius, G. and O’Dowd, C. D.: Effects of continental  
1120 boundary layer evolution, convection, turbulence and entrainment, on aerosol formation, *Tellus*,  
1121 *Ser. B Chem. Phys. Meteorol.*, 53(4), 441–461, doi:10.3402/tellusb.v53i4.16617, 2001.  
1122  
1123 Olin, M., Kuuluvainen, H., Aurela, M., Kalliokoski, J., Kuittinen, N., Isotalo, M., Timonen, H. J.,  
1124 Niemi, J. V., Rönkkö, T. and Dal Maso, M.: Traffic-originated nanocluster emission exceeds  
1125 H<sub>2</sub>SO<sub>4</sub>-driven photochemical new particle formation in an urban area, *Atmos. Chem. Phys.*, 20(1),  
1126 1–13, doi:10.5194/acp-20-1-2020, 2020.  
1127  
1128 Ortega, I. K., Kurtén, T., Vehkamäki, H. and Kulmala, M.: The role of ammonia in sulfuric acid ion  
1129 induced nucleation, *Atmos. Chem. Phys.*, 8(11), 2859–2867, doi:10.5194/acp-8-2859-2008, 2008.  
1130  
1131 Park, M., Yum, S. S. and Kim, J. H.: Characteristics of submicron aerosol number size distribution  
1132 and new particle formation events measured in Seoul, Korea, during 2004–2012, *Asia-Pacific J.*  
1133 *Atmos. Sci.*, 51(1), 1–10, doi:10.1007/s13143-014-0055-0, 2015.  
1134  
1135 Peng, Y., Dong, Y., Li, X., Liu, X., Dai, J., Chen, C., Dong, Z., Du, C. and Wang, Z.: Different  
1136 characteristics of new particle formation events at two suburban sites in northern China,  
1137 *Atmosphere*, 8, 258, doi:10.3390/atmos8120258, 2017.  
1138  
1139 Petäjä, T., Mauldin, R. L., Kosciuch, E., McGrath, J., Nieminen, T., Paasonen, P., Boy, M.,  
1140 Adamov, A., Kotiaho, T. and Kulmala, M.: Sulfuric acid and OH concentrations in a boreal forest  
1141 site, *Atmos. Chem. Phys.*, 9(19), 7435–7448, doi:10.5194/acp-9-7435-2009, 2009.  
1142

1143 Poling, B. E., Prausnitz, J. M. and O'Connell, J. P.: The properties of gases and liquids, 5th Ed.,  
1144 McGraw-Hill Education, New York, USA, 768 pp., 2001.  
1145  
1146 Politis, M., Pilinis, C. and Lekkas, T. D.: Ultrafine particles (UFP) and health effects. Dangerous.  
1147 Like no other PM? Review and analysis, *Glob. Nest J.*, 10(3), 439–452, 2008.  
1148  
1149 Querol, X., Gangoiti, G., Mantilla, E., Alastuey, A., Minguillón, M. C., Amato, F., Reche, C.,  
1150 Viana, M., Moreno, T., Karanasiou, A., Rivas, I., Pérez, N., Ripoll, A., Brines, M., Ealo, M.,  
1151 Pandolfi, M., Lee, H. K., Eun, H. R., Park, Y. H., Escudero, M., Beddows, D., Harrison, R. M.,  
1152 Bertrand, A., Marchand, N., Lyasota, A., Codina, B., Olid, M., Udina, M., Jiménez-Esteve, B. B.,  
1153 Jiménez-Esteve, B. B., Alonso, L., Millán, M. and Ahn, K. H.: Phenomenology of high-ozone  
1154 episodes in NE Spain, *Atmos. Chem. Phys.*, 17(4), 2817–2838, doi:10.5194/acp-17-2817-2017,  
1155 2017.  
1156  
1157 Riccobono, F., Schobesberger, S., Scott, C. E., Dommen, J., Ortega, I. K., Rondo, L., Almeida, J.,  
1158 Amorim, A., Bianchi, F., Breitenlechner, M., David, A., Downard, A., Dunne, E. M., Duplissy, J.,  
1159 Ehrhart, S., Flagan, R. C., Franchin, A., Hansel, A., Junninen, H., Kajos, M., Keskinen, H., Kupc,  
1160 A., Makhmutov, V., Mathot, S., Nieminen, T., Onnela, A., Petäjä, T., Tsagkogeorgas, G.,  
1161 Vaattovaara, P., Viisanen, Y., Vrtala, A. and Wagner, P. E.: Oxidation Products of Biogenic  
1162 Atmospheric Particles, *Science*, 717, 717–722, doi:10.1126/science.1243527, 2014.  
1163  
1164 Riipinen, I., Sihto, S.-L. L., Kulmala, M., Arnold, F., Dal Maso, M., Birmili, W., Saarnio, K.,  
1165 Teinilä, K., Kerminen, V.-M. M., Laaksonen, A. and Lehtinen, K. E. J. J.: Connections between  
1166 atmospheric sulphuric acid and new particle formation during QUEST III–IV campaigns in  
1167 Heidelberg and Hyytiälä, *Atmos. Chem. Phys. Atmos. Chem. Phys.*, 7(8), 1899–1914,  
1168 doi:10.5194/acp-7-1899-2007, 2007.  
1169  
1170 Rimnácová, D., Ždímal, V., Schwarz, J., Smolík, J. and Rimnác, M.: Atmospheric aerosols in  
1171 suburb of Prague: The dynamics of particle size distributions, *Atmos. Res.*, 101(3), 539–552,  
1172 doi:10.1016/j.atmosres.2010.10.024, 2011.  
1173  
1174 Rivas, I., Beddows, D. C. S., Amato, F., Green, D. C., Järvi, L., Hueglin, C., Reche, C., Timonen,  
1175 H., Fuller, G. W., Niemi, J. V., Pérez, N., Aurela, M., Hopke, P. K., Alastuey, A., Kulmala, M.,  
1176 Harrison, R. M., Querol, X. and Kelly, F. J.: Source apportionment of particle number size  
1177 distribution in urban background and traffic stations in four European cities, *Environ. Int.*, 135,  
1178 105345, doi:10.1016/j.envint.2019.105345, 2020.  
1179  
1180 Rodríguez, S., Querol, X., Alastuey, A., Kallos, G. and Kakaliagou, O.: Saharan dust contributions  
1181 to PM10 and TSP levels in Southern and Eastern Spain, *Atmos. Environ.*, 35(14), 2433–2447,  
1182 doi:10.1016/S1352-2310(00)00496-9, 2001.

1183 Rönkkö, T., Kuuluvainen, H., Karjalainen, P., Keskinen, J., Hillamo, R., Niemi, J. V., Pirjola, L.,  
1184 Timonen, H. J., Saarikoski, S., Saukko, E., Järvinen, A., Silvennoinen, H., Rostedt, A., Olin, M.,  
1185 Yli-Ojanperä, J., Nousiainen, P., Kousa, A. and Dal Maso, M.: Traffic is a major source of  
1186 atmospheric nanocluster aerosol, *Proc. Natl. Acad. Sci.*, 114(29), 7549–7554,  
1187 doi:10.1073/pnas.1700830114, 2017.  
1188  
1189 Salma, I., Németh, Z., Kerminen, V. M., Aalto, P., Nieminen, T., Weidinger, T., Molnár, Á., Imre,  
1190 K. and Kulmala, M.: Regional effect on urban atmospheric nucleation, *Atmos. Chem. Phys.*, 16(14),  
1191 8715–8728, doi:10.5194/acp-16-8715-2016, 2016.  
1192  
1193 Salma, I., Borsós, T., Németh, Z., Weidinger, T., Aalto, P. and Kulmala, M.: Comparative study of  
1194 ultrafine atmospheric aerosol within a city, *Atmos. Environ.*, 92, 154–161,  
1195 doi:10.1016/j.atmosenv.2014.04.020, 2014.  
1196  
1197 Sarnela, N., Jokinen, T., Nieminen, T., Lehtipalo, K., Junninen, H., Kangasluoma, J., Hakala, J.,  
1198 Taipale, R., Larnimaa, K., Westerholm, H., Schobesberger, S., Sipil, M., Heijari, J., Kerminen, V.  
1199 and Pet, T.: Sulphuric acid and aerosol particle production in the vicinity of an oil refinery, *Atmos.*  
1200 *Environ.*, 119, 156–166, doi:10.1016/j.atmosenv.2015.08.033, 2015.  
1201  
1202 Schobesberger, S., Franchin, A., Bianchi, F., Rondo, L., Duplissy, J., Kürten, A., Ortega, I. K.,  
1203 Metzger, A., Schnitzhofer, R., Almeida, J., Amorim, A., Dommen, J., Dunne, E. M., Ehn, M.,  
1204 Gagné, S., Ickes, L., Junninen, H., Hansel, A., Kerminen, V. M., Kirkby, J., Kupc, A., Laaksonen,  
1205 A., Lehtipalo, K., Mathot, S., Onnela, A., Petäjä, T., Riccobono, F., Santos, F. D., Sipilä, M., Tomé,  
1206 A., Tsagkogeorgas, G., Viisanen, Y., Wagner, P. E., Wimmer, D., Curtius, J., Donahue, N. M.,  
1207 Baltensperger, U., Kulmala, M. and Worsnop, D. R.: On the composition of ammonia-sulfuric-acid  
1208 ion clusters during aerosol particle formation, *Atmos. Chem. Phys.*, 15(1), 55–78, doi:10.5194/acp-  
1209 15-55-2015, 2015.  
1210  
1211 Seinfeld, J. H. and Pandis, S. N.: *Atmospheric Chemistry and Physics: From Air Pollution to*  
1212 *Climate Change*, 3rd Editio., John Wiley & Sons, Inc, New Jersey, Canada, 2012.  
1213  
1214 Shen, X., Sun, J., Kivekäs, N., Kristensson, A., Zhang, X., Zhang, Y., Zhang, L., Fan, R., Qi, X.,  
1215 Ma, Q. and Zhou, H.: Spatial distribution and occurrence probability of regional new particle  
1216 formation events in eastern China, *Atmos. Chem. Phys.*, 18(2), 587–599, doi:10.5194/acp-18-587-  
1217 2018, 2018.  
1218  
1219 Shi, J. P., Evans, D. E., Khan, A. A. and Harrison, R. M.: Sources and concentration of  
1220 nanoparticles (10 nm diameter) in the urban atmosphere, *Atmos. Environ.*, 35, 1193–1202,  
1221 doi.org/10.1016/S1352-2310(00)00418-0, 2001.  
1222

1223 Siakavaras, D., Samara, C., Petrakakis, M. and Biskos, G.: Nucleation events at a coastal city  
1224 during the warm period: Kerbside versus urban background measurements, *Atmos. Environ.*, 140,  
1225 60–68, doi:10.1016/j.atmosenv.2016.05.054, 2016.  
1226  
1227 Sipila, M., Berndt, T., Petaja, T., Brus, D., Vanhanen, J., Stratmann, F., Patokoski, J., Mauldin III,  
1228 R. L., Hyvarinen, A. P., Lihavainen, H. and Kulmala, M.: The role of sulfuric acid in atmospheric  
1229 nucleation, *Science*, 327, 1243–1246, doi:10.1126/science.1180315, 2010.  
1230  
1231 Spracklen, D. V., Carslaw, K. S., Kulmala, M., Kerminen, V. M., Sihto, S. L., Riipinen, I.,  
1232 Merikanto, J., Mann, G. W., Chipperfield, M. P., Wiedensohler, A., Birmili, W. and Lihavainen, H.:  
1233 Contribution of particle formation to global cloud condensation nuclei concentrations, *Geophys.*  
1234 *Res. Lett.*, 35(6), 1–5, doi:10.1029/2007GL033038, 2008.  
1235  
1236 Stafoggia, M., Schneider, A., Cyrus, J., Samoli, E., Andersen, Z.J., Bedada, G.B., Bellander, T.,  
1237 Cattani, G., Eleftheriadis, K., Faustini, A., Hoffmann, B., Jacquemin, B., Katsouyanni, K.,  
1238 Massling, A., Pekkanen, J., Perez, N., Peters, A., Quass, U., Yli-Tuomi, T., Forastiere, F.:  
1239 Association between short-term exposure to ultrafine particles and mortality in eight European  
1240 Urban areas. *Epidemiology* 28 (2),172–180. <https://doi.org/10.1097/EDE.0000000000000599>.  
1241 2017.  
1242  
1243 Stanier, C. O., Khlystov, A. Y. and Pandis, S. N.: Nucleation events during the Pittsburgh Air  
1244 Quality Study: Description and relation to key meteorological, gas phase, and aerosol parameters,  
1245 *Aerosol Sci. Technol.*, 38, 253–264, doi:10.1080/02786820390229570, 2004.  
1246  
1247 Stojiljkovic, A., Kauhaniemi, M., Kukkonen, J., Kupiainen, K., Karppinen, A., Rolstad Denby, B.,  
1248 Kousa, A., Niemi, J. V. and Ketzel, M.: The impact of measures to reduce ambient air PM10  
1249 concentrations originating from road dust, evaluated for a street canyon in Helsinki, *Atmos. Chem.*  
1250 *Phys.*, 19(17), 11199–11212, doi:10.5194/acp-19-11199-2019, 2019.  
1251  
1252 Sun, J., Birmili, W., Hermann, M., Tuch, T., Weinhold, K., Spindler, G.,Schladitz, A., Bastian, S.,  
1253 Löschau, G., Cyrus, J., Gu, J., Flentje, H., Briel, B., Asbach, C., Kaminski, H.,Ries, L., Sohmer, R.,  
1254 Gerwig, H., Wirtz, K., Meinhardt, F., Schwerin, A., Bath, O., Ma, N., Wiedensohler,A.: Variability  
1255 of Black Carbon mass concentrations, sub-micrometer particle number concentrations and size  
1256 distributions: Results of the German Ultrafine Aerosol Network ranging from city street to high  
1257 Alpine locations, *Atmos. Environ.*, 202, 256-268, 2019.  
1258  
1259 Tobías, A., Rivas, I., Reche, C., Alastuey, A., Rodríguez, S., Fernández-camacho, R., Sánchez, A.  
1260 M., Campa, D., De, J., Sunyer, J. and Querol, X.: Short-term effects of ultra fine particles on daily  
1261 mortality by primary vehicle exhaust versus secondary origin in three Spanish cities, *Environ. Int.*,  
1262 111, 144–151, doi:10.1016/j.envint.2017.11.015, 2018.

1263  
1264 Tröstl, J., Chuang, W. K., Gordon, H., Heinritzi, M., Yan, C., Molteni, U., Ahlm, L., Frege, C.,  
1265 Bianchi, F., Wagner, R., Simon, M., Lehtipalo, K., Williamson, C., Craven, J. S., Duplissy, J.,  
1266 Adamov, A., Almeida, J., Bernhammer, A. K., Breitenlechner, M., Brilke, S., Dias, A., Ehrhart, S.,  
1267 Flagan, R. C., Franchin, A., Fuchs, C., Guida, R., Gysel, M., Hansel, A., Hoyle, C. R., Jokinen, T.,  
1268 Junninen, H., Kangasluoma, J., Keskinen, H., Kim, J., Krapf, M., Kürten, A., Laaksonen, A.,  
1269 Lawler, M., Leiminger, M., Mathot, S., Möhler, O., Nieminen, T., Onnela, A., Petäjä, T., Piel, F.  
1270 M., Miettinen, P., Rissanen, M. P., Rondo, L., Sarnela, N., Schobesberger, S., Sengupta, K., Sipilä,  
1271 M., Smith, J. N., Steiner, G., Tomè, A., Virtanen, A., Wagner, A. C., Weingartner, E., Wimmer, D.,  
1272 Winkler, P. M., Ye, P., Carslaw, K. S., Curtius, J., Dommen, J., Kirkby, J., Kulmala, M., Riipinen,  
1273 I., Worsnop, D. R., Donahue, N. M. and Baltensperger, U.: The role of low-volatility organic  
1274 compounds in initial particle growth in the atmosphere, *Nature*, 533(7604), 527–531,  
1275 doi:10.1038/nature18271, 2016.  
1276  
1277 Voigtländer, J., Tuch, T., Birmili, W. and Wiedensohler, A.: Correlation between traffic density and  
1278 particle size distribution in a street canyon and the dependence on wind direction, *Atmos. Chem.*  
1279 *Phys.*, 6(12), 4275–4286, doi:10.5194/acp-6-4275-2006, 2006.  
1280  
1281 Vratolis, S., Gini, M. I., Bezantakos, S., Stavroulas, I., Kalivitis, N., Kostenidou, E., Louvaris, E.,  
1282 Siakavaras, D., Biskos, G., Mihalopoulos, N., Pandis, S. N. N., Pilinis, C., Papayannis, A. and  
1283 Eleftheriadis, K.: Particle number size distribution statistics at City-Centre Urban Background,  
1284 urban background, and remote stations in Greece during summer, *Atmos. Environ.*, 213, 711–726,  
1285 doi:10.1016/j.atmosenv.2019.05.064, 2019.  
1286  
1287 Vrekoussis, M., Richter, A., Hilboll, A., Burrows, J. P., Gerasopoulos, E., Lelieveld, J., Barrie, L.,  
1288 Zerefos, C. and Mihalopoulos, N.: Economic crisis detected from space: Air quality observations  
1289 over Athens/Greece, *Geophys. Res. Lett.*, 40(2), 458–463, doi:10.1002/grl.50118, 2013.  
1290  
1291 Wang, Z., Wu, Z., Yue, D., Shang, D., Guo, S., Sun, J., Ding, A., Wang, L., Jiang, J., Guo, H., Gao,  
1292 J., Cheung, H. C., Morawska, L., Keywood, M. and Hu, M.: New particle formation in China:  
1293 Current knowledge and further directions, *Sci. Total Environ.*, 577, 258–266,  
1294 doi:10.1016/j.scitotenv.2016.10.177, 2017.  
1295  
1296 Wang, D., Guo, H., Cheung, K. and Gan, F.: Observation of nucleation mode particle burst and new  
1297 particle formation events at an urban site in Hong Kong, *Atmos. Environ.*, 99, 196–205,  
1298 doi:10.1016/j.atmosenv.2014.09.074, 2014.  
1299  
1300 Wang, F., Zhang, Z., Massling, A., Ketznel, M. and Kristensson, A.: Particle formation events  
1301 measured at a semirural background site in Denmark, *Environ. Sci. Pollut. Res.*, 20(5), 3050–3059,  
1302 doi:10.1007/s11356-012-1184-6, 2013.

1303  
1304 Wang, F., Ketzel, M., Ellermann, T., Wählén, P., Jensen, S. S., Fang, D. and Massling, A.: Particle  
1305 number, particle mass and NO<sub>x</sub> emission factors at a highway and an urban street in Copenhagen,  
1306 *Atmos. Chem. Phys.*, 10(6), 2745–2764, doi:10.5194/acp-10-2745-2010, 2010.  
1307  
1308 Weber, R. J., McMurry, P. H., Mauldin, L., Tanner, D. J., Eisele, F. L., Brechtel, F. J., Kreidenweis,  
1309 S. M., Kok, G. L., Schillawski, R. D., Baumgardner, D. and Baumgardner, B.: A study of new  
1310 particle formation and growth involving biogenic and trace gas species measured during ACE 1, *J.*  
1311 *Geophys. Res. Atmos.*, 103(D13), 16385–16396, doi:10.1029/97JD02465, 1998.  
1312  
1313 Weber, R. J., McMurry, P. H., Eisele, F. L. and Tanner, D. J.: Measurement of expected nucleation  
1314 precursor species and 3-500-nm diameter particles at Mauna Loa Observatory, Hawaii, *J. Atmos.*  
1315 *Sci.*, 52(12), 2242–2257, 1995.  
1316  
1317 Wehner, B., Siebert, H., Stratmann, F., Tuch, T., Wiedensohler, A., Petäjä, T., Dal Maso, M. and  
1318 Kulmala, M.: Horizontal homogeneity and vertical extent of new particle formation events, *Tellus,*  
1319 *Ser. B Chem. Phys. Meteorol.*, 59(3), 362–371, doi:10.1111/j.1600-0889.2007.00260.x, 2007.  
1320  
1321 Wonaschütz, A., Demattio, A., Wagner, R., Burkart, J., Zíková, N., Vodička, P., Ludwig, W.,  
1322 Steiner, G., Schwarz, J. and Hitzenberger, R.: Seasonality of new particle formation in Vienna,  
1323 Austria - Influence of air mass origin and aerosol chemical composition, *Atmos. Environ.*, 118,  
1324 118–126, doi:10.1016/j.atmosenv.2015.07.035, 2015.  
1325  
1326 Woo, K. S., Chen, D. R., Pui, D. Y. H. H. and McMurry, P. H.: Measurement of Atlanta aerosol  
1327 size distributions: Observations of lutrafine particle events, *Aerosol Sci. Technol.*, 34, 75–87,  
1328 doi:10.1080/02786820120056, 2001.  
1329  
1330 Xiao, S., Wang, M. Y., Yao, L., Kulmala, M., Zhou, B., Yang, X., Chen, J. M., Wang, D. F., Fu, Q.  
1331 Y., Worsnop, D. R. and Wang, L.: Strong atmospheric new particle formation in winter in urban  
1332 Shanghai, China, *Atmos. Chem. Phys.*, 15(4), 1769–1781, doi:10.5194/acp-15-1769-2015, 2015.  
1333  
1334 Yao, L., Garmash, O., Bianchi, F., Zheng, J., Yan, C., Kontkanen, J., Junninen, H., Mazon, S. B.,  
1335 Ehn, M., Paasonen, P., Sipilä, M., Wang, M., Wang, X., Xiao, S., Chen, H., Lu, Y., Zhang, B.,  
1336 Wang, D., Fu, Q., Geng, F., Li, L., Wang, H., Qiao, L., Yang, X., Chen, J., Kerminen, V. M.,  
1337 Petäjä, T., Worsnop, D. R., Kulmala, M. and Wang, L.: Atmospheric new particle formation from  
1338 sulfuric acid and amines in a Chinese megacity, *Science*, 361(6399), 278–281,  
1339 doi:10.1126/science.aao4839, 2018.  
1340  
1341 Yli-Juuti, T., Nieminen, T., Hirsikko, A., Aalto, P. P., Asmi, E., Hörrak, U., Manninen, H. E.,  
1342 Patokoski, J., Dal Maso, M., Petäjä, T., Rinne, J., Kulmala, M. and Riipinen, I.: Growth rates of



1343 nucleation mode particles in Hyytiälä during 2003-2009: Variation with particle size, season, data  
1344 analysis method and ambient conditions, *Atmos. Chem. Phys.*, 11(24), 12865–12886,  
1345 doi:10.5194/acp-11-12865-2011, 2011.  
1346 YΠIEKA (Ministry for the Environment, Energy and Climate Change in Greece): Annual report of  
1347 atmospheric pollution 2011, Ministry for the Environment, Energy and Climate Change in Greece,  
1348 Department of Air Quality, April 2012,  
1349 <http://www.ypeka.gr/LinkClick.aspx?fileticket=TYgrT0qoSrI%3D&tabid=490&language=el-GR>,  
1350 last accessed 18/9/2019, 2012.  
1351  
1352 Ždímal, V., Smolík, J., Eleftheriadis, K., Wagner, Z., Housiadas, C., Mihalopoulos, N., Mikuška,  
1353 P., Večeřa, Z., Kopanakis, I. and Lazaridis, M.: Dynamics of atmospheric aerosol number size  
1354 distributions in the eastern Mediterranean during the “SUB-AERO” project, *Water, Air, Soil*  
1355 *Pollut.*, 214(1–4), 133–146, doi:10.1007/s11270-010-0410-4, 2011.  
1356

1357 **TABLE LEGENDS:**

1358

1359 **Table 1:** Location and data availability (seasonal data availability is found in Table S4) of the  
1360 sites in the present. In the studies referenced an extended description of the sites can be  
1361 found.

1362

1363

1364 **FIGURE LEGENDS**

1365

1366 **Figure 1:** Map of the areas of study.

1367

1368 **Figure 2:** Frequency (a) and seasonal variation (b) of New Particle Formation events (Winter – DJF;  
1369 Spring – MAM; Summer – JJA; Autumn – SON).

1370 **Figure 3:** Ratio of New Particle Formation event probability between weekends to weekdays. The  
1371 greater the ratio the more probable it is for an event to take place during weekends  
1372 compared to weekdays.

1373 **Figure 4:** Growth rate of particles up to 30 nm (with standard deviations) during New Particle  
1374 Formation events at all sites.

1375 **Figure 5:** Seasonal variation of growth rate of particles up to 30 nm on New Particle Formation at  
1376 (a) the rural background, (b) urban background and (c) roadside sites.

1377 **Figure 6:** Formation rate of 10 nm particles ( $J_{10}$ ) (with standard deviations) from New Particle  
1378 Formation at all sites.

1379 **Figure 7:** Seasonal variation of formation rate of 10 nm particles ( $J_{10}$ ) (with standard deviations)  
1380 from New Particle Formation events at (a) the rural background, (b) urban background  
1381 and (c) roadside sites.

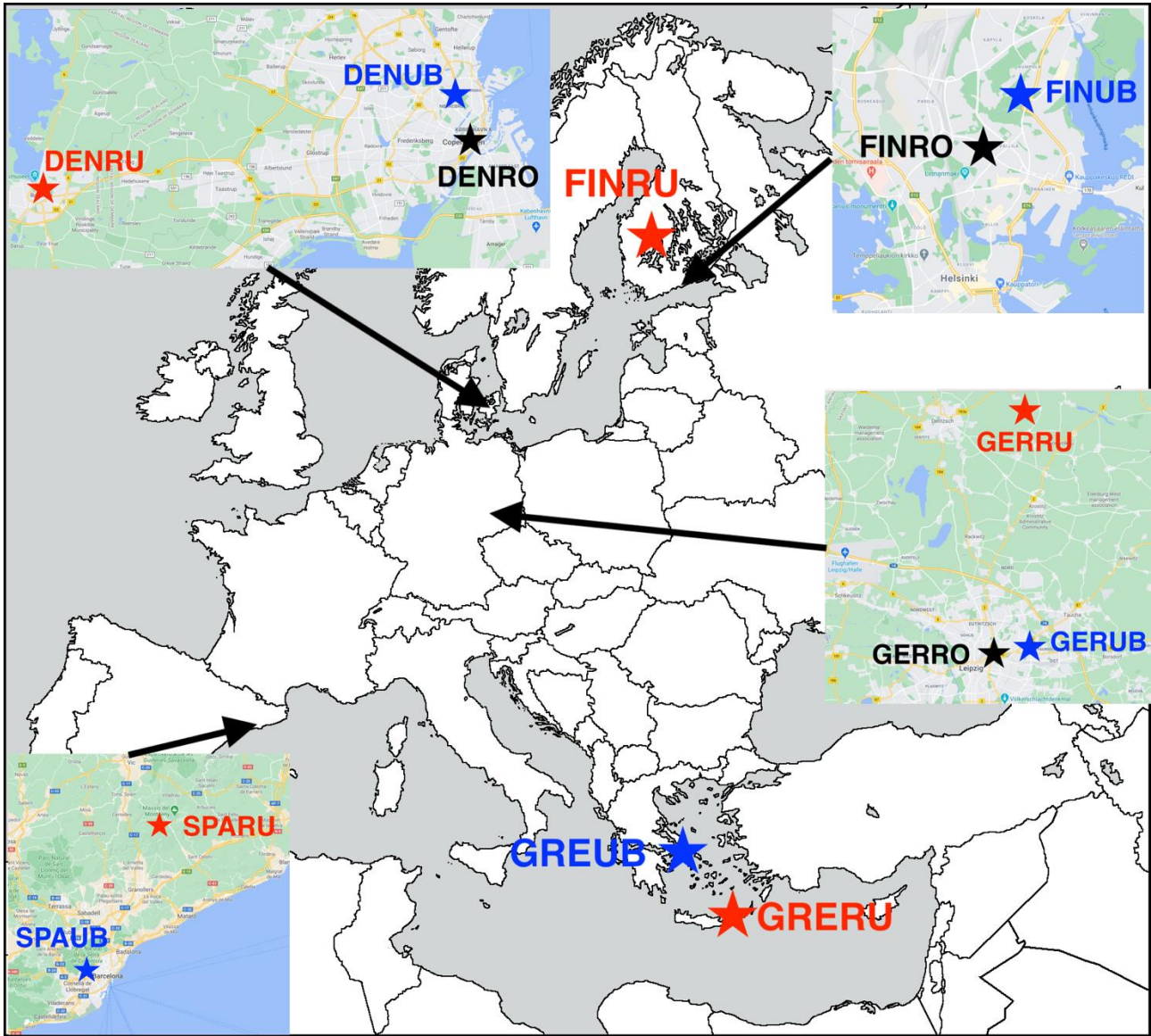
1382 **Figure 8:** (a) Number of region-wide New Particle Formation events per season and (b) fraction of  
1383 region-wide events to total New Particle Formation events per season for each site.  
1384 Region-wide events are considered those that occur on the same day on both background  
1385 sites (Rural and Urban background).

1386 **Figure 9:** (a)  $NSF_{NUC}$  (average relative increase of ultrafine particles – particles of diameter up to  
1387 100 nm) due to New Particle Formation events on event days) and (b)  $NSF_{GEN}$  (average  
1388 annual relative increase of ultrafine particles due to New Particle Formation events) at all  
1389 sites.

1390 **Table 1:** Location and data availability (seasonal data availability is found in Table S4) of the sites in the present study. In the studies referenced an extended description of the sites can be found.

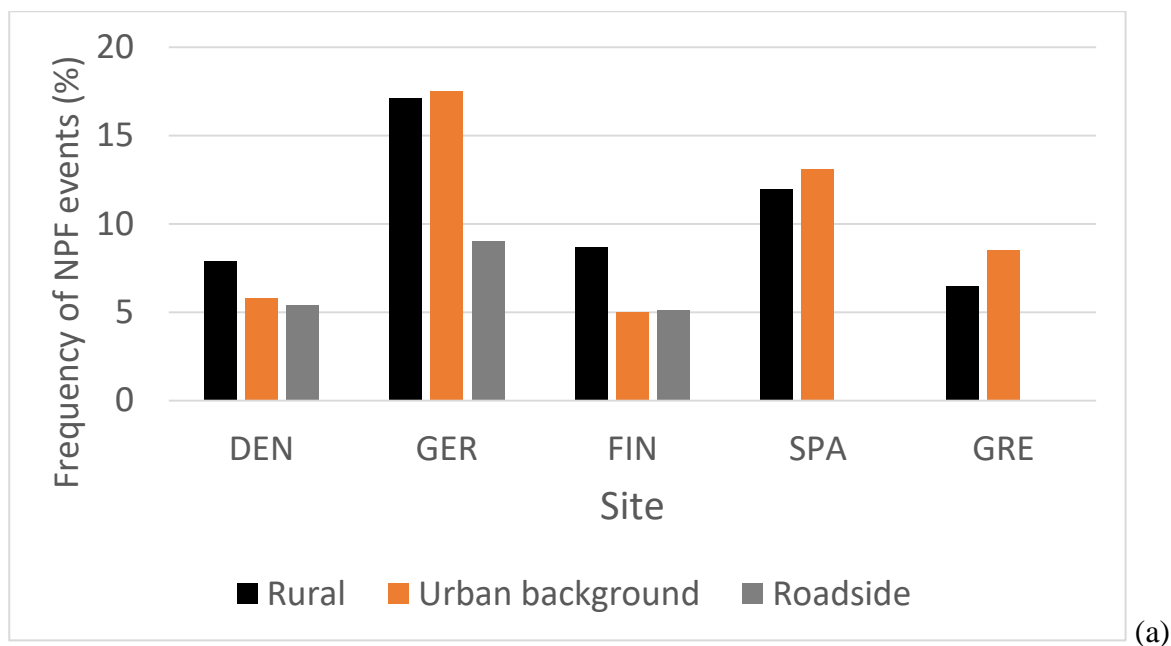
Site	Location	Available data	Meteorological data location	Data availability	Reference
DENRU	Lille Valby, 25 km W of Copenhagen, (55° 41' 41" N; 12° 7' 7" E) (2008 – 6/2010) Risø, 7 km north of Lille Valby, (55° 38' 40" N; 12° 5' 19" E) (7/2010 – 2017)	DMPS and CPC (5.8 - 700 nm, 65.4% availability), NO, NO <sub>x</sub> , SO <sub>2</sub> , O <sub>3</sub> , minerals, OC, EC, NO <sub>3</sub> <sup>-</sup> , SO <sub>4</sub> <sup>2-</sup> , NH <sub>4</sub> <sup>+</sup>	Ørsted – Institute station	2008 – 2017	Ketzel et al., 2004
DENUB	Ørsted - Institute, 2 km NE of the city centre, Copenhagen, Denmark (55° 42' 1" N; 12° 33' 41" E)	DMPS and CPC (5.8 - 700 nm, 59.0% availability), NO, NO <sub>x</sub> , O <sub>3</sub> , minerals, EC	On site	2008 – 2017	Wang et al., 2010
DENRO	H.C. Andersens Boulevard, Copenhagen, Denmark (55° 40' 28" N; 12° 34' 16" E)	DMPS and CPC (5.8 - 700 nm, 65.0% availability), NO, NO <sub>x</sub> , SO <sub>2</sub> , O <sub>3</sub> , minerals, OC, EC, NO <sub>3</sub> <sup>-</sup> , SO <sub>4</sub> <sup>2-</sup> , NH <sub>4</sub> <sup>+</sup>	Ørsted – Institute station	2008 – 2017	Wang et al., 2010
GERRU	Melpitz, 40 km NE of Leipzig, Germany (51° 31' 31.85" N; 12° 26' 40.30" E)	TDMPS with CPC (4.8 - 800 nm, 87.1% availability), OC, NO <sub>3</sub> <sup>-</sup> , SO <sub>4</sub> <sup>2-</sup> , NH <sub>4</sub> <sup>+</sup> , Cl <sup>-</sup>	On site	2008 – 2011	Birmili et al., 2016
GERUB	Tropos, 3 km NE from the city centre of Leipzig, Germany (51° 21' 9.1" N; 12° 26' 5.1" E)	TDMPS with CPC (3 - 800 nm, 88.0% availability)	On site	2008 – 2011	Birmili et al., 2016
GERRO	Eisenbahnstraße, Leipzig, Germany (51° 20' 43.80" N; 12° 24' 28.35" E)	TDMPS with CPC (4 - 800 nm, 64.4% availability)	Tropos station	2008 – 2011	Birmili et al., 2016
FINRU	Hyytiälä, 250 km N of Helsinki, Finland (61° 50' 50.70" N; 24° 17' 41.20" E)	TDMPS with CPC (3 – 1000 nm, 98.7% availability), NO, NO <sub>x</sub> , SO <sub>2</sub> , O <sub>3</sub> , CO, CH <sub>4</sub> , VOCs, H <sub>2</sub> SO <sub>4</sub>	On site	2008 – 2011 & 2015 – 2018	Aalto et al., 2001
FINUB	Kumpula Campus 4 km N of the city centre, Helsinki, Finland (60° 12' 10.52" N; 24° 57' 40.20" E)	TDMPS with CPC (3.4 - 1000 nm, 94.0% availability)	On site	2008 – 2011 & 2015 – 2018	Järvi et al., 2009
FINRO	Mäkelänkatu street, Helsinki, Finland (60° 11' 47.57" N; 24° 57' 6.01" E)	DMPS (6 - 800 nm, 90.0% availability), NO, NO <sub>2</sub> , NO <sub>x</sub> , O <sub>3</sub> , BC and SO <sub>2</sub> from Kalio Station	Pasila station and on site	2015 – 2018	Hietikko et al., 2018
SPARU	Montseny, 50 km NNE from Barcelona, Spain (41° 46' 45" N; 2° 21' 29" E)	SMPS (9 – 856 nm, 47.7% availability), NO, NO <sub>2</sub> , SO <sub>2</sub> , O <sub>3</sub> , CO, OM, SO <sub>4</sub> <sup>2-</sup>	On site	2012 - 2015	Dall'Osto et al., 2013
SPAUB	Palau Reial, Barcelona, Spain (41° 23' 14" N; 2° 6' 56" E)	SMPS (10.9 – 478 nm, 64.2% availability), NO, NO <sub>2</sub> , SO <sub>2</sub> , O <sub>3</sub> , CO, BC, OM, SO <sub>4</sub> <sup>2-</sup> , PM <sub>2.5</sub> , PM <sub>10</sub>	On site	2012 – 2015	Dall'Osto et al., 2012

GRERU	Finokalia, 70 km E of Heraklion, Greece (35° 20' 16.8" N; 25° 40' 8.4" E)	SMPS (8.77 - 849 nm, 92.4% availability), NO, NO <sub>2</sub> , O <sub>3</sub> , OC, EC	On site	2012 – 2018	Kalkavouras et al., 2017
GREUB	“Demokritos”, 12 km NE from the city centre, Athens, Greece (37° 59' 41.96" N; 23° 48' 57.56" E)	SMPS (10 – 550 nm, 77.2% availability)	On site	2015 – 2018	Stafogia et al., 2005

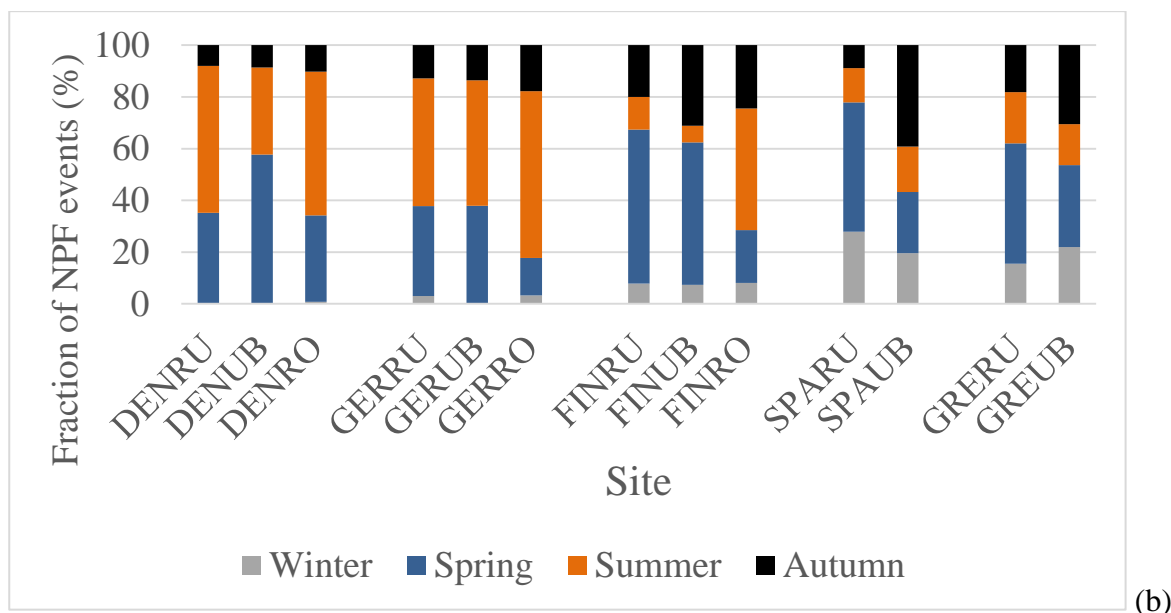


1395 **Figure 1:** Map of the areas of study.

1400

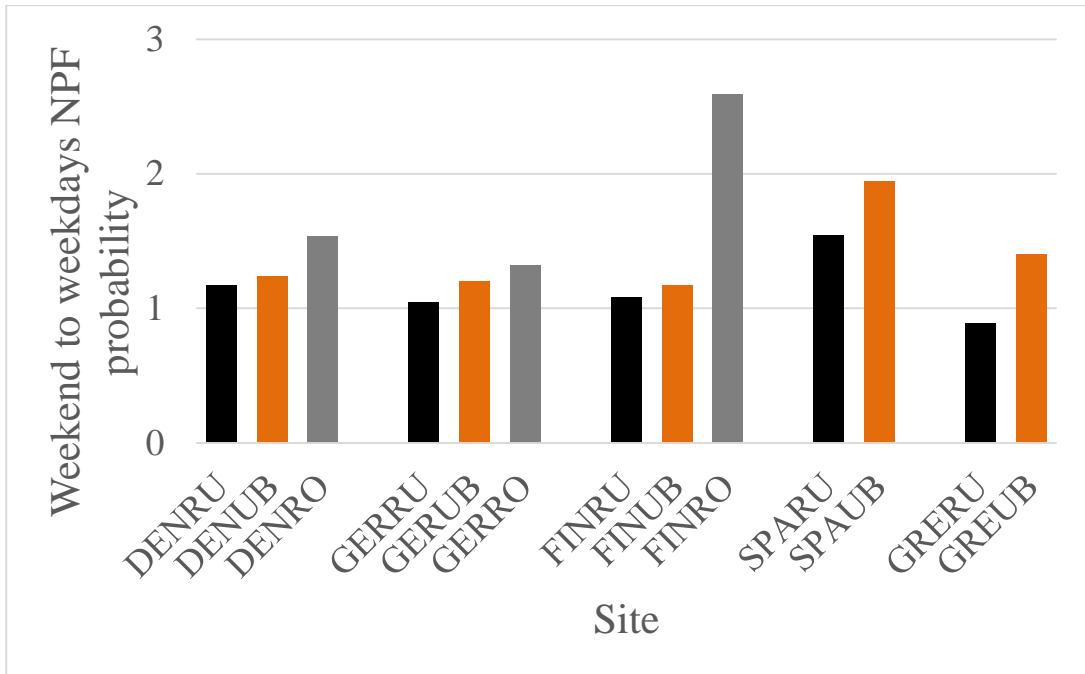


(a)

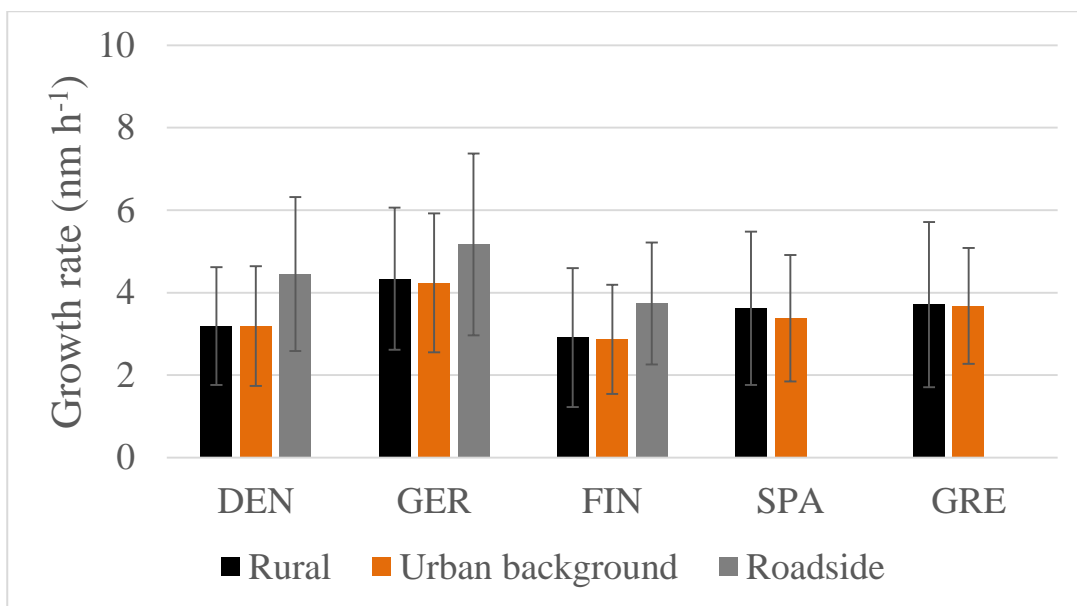


(b)

**Figure 2:** Frequency (a) and seasonal variation (b) of New Particle Formation events (Winter – DJF; 1405 Spring – MAM; Summer – JJA; Autumn – SON).



1410 **Figure 3:** Ratio of New Particle Formation event probability between weekends to weekdays. The greater the ratio the more probable it is for an event to take place during weekends compared to weekdays.

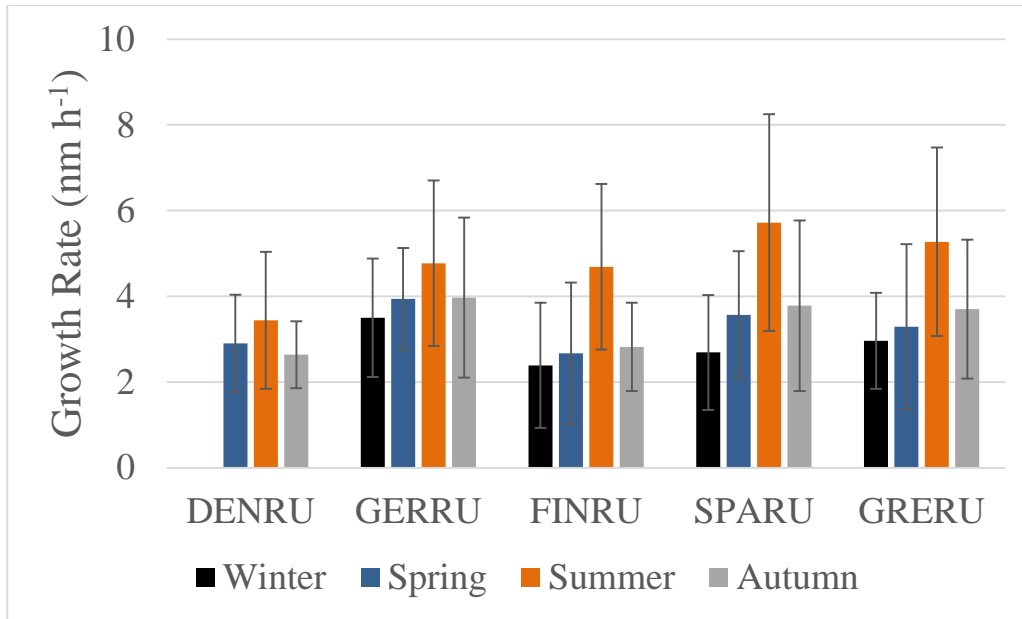


1415

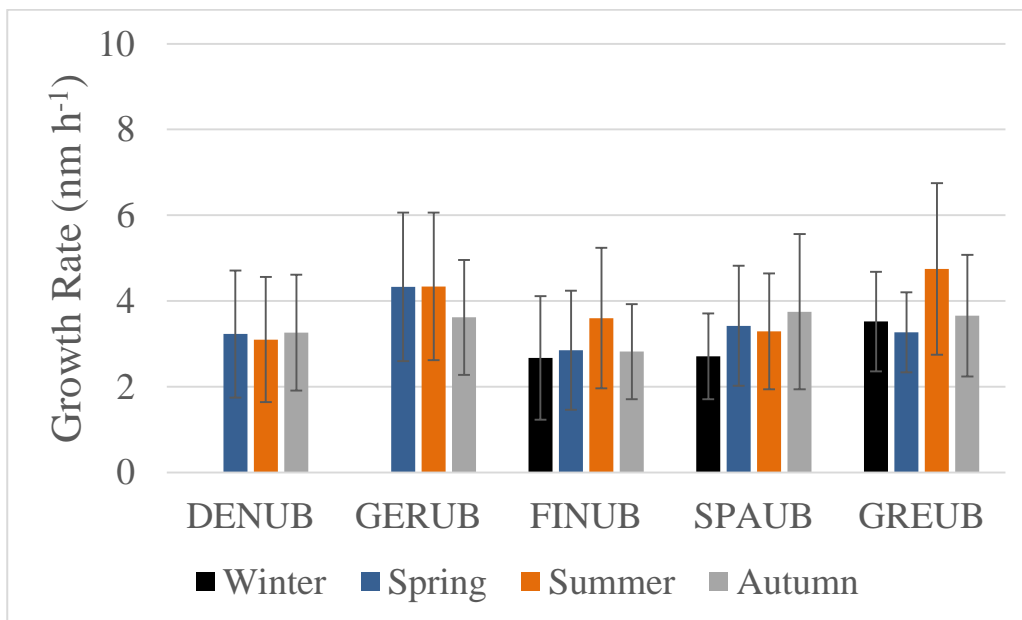
**Figure 4:** Growth rate of particles up to 30 nm (with standard deviations) during New Particle Formation events at all sites.



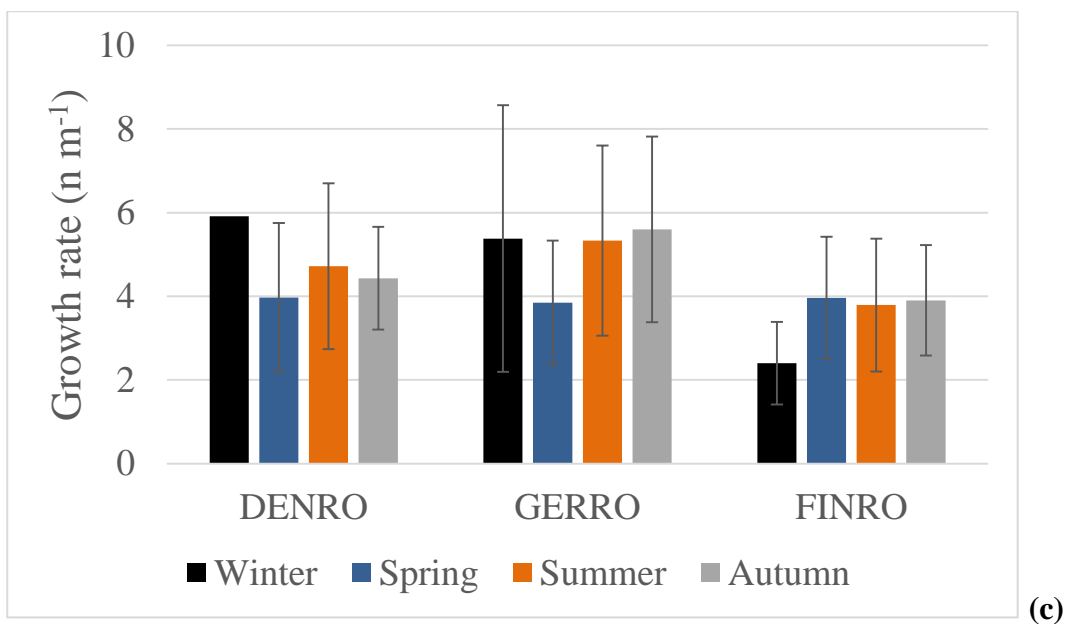
1420



(a)



(b)



1425 **Figure 5:** Seasonal variation of growth rate of particles up to 30 nm on New Particle Formation at (a) the rural background, (b) urban background and (c) roadside sites.

1430

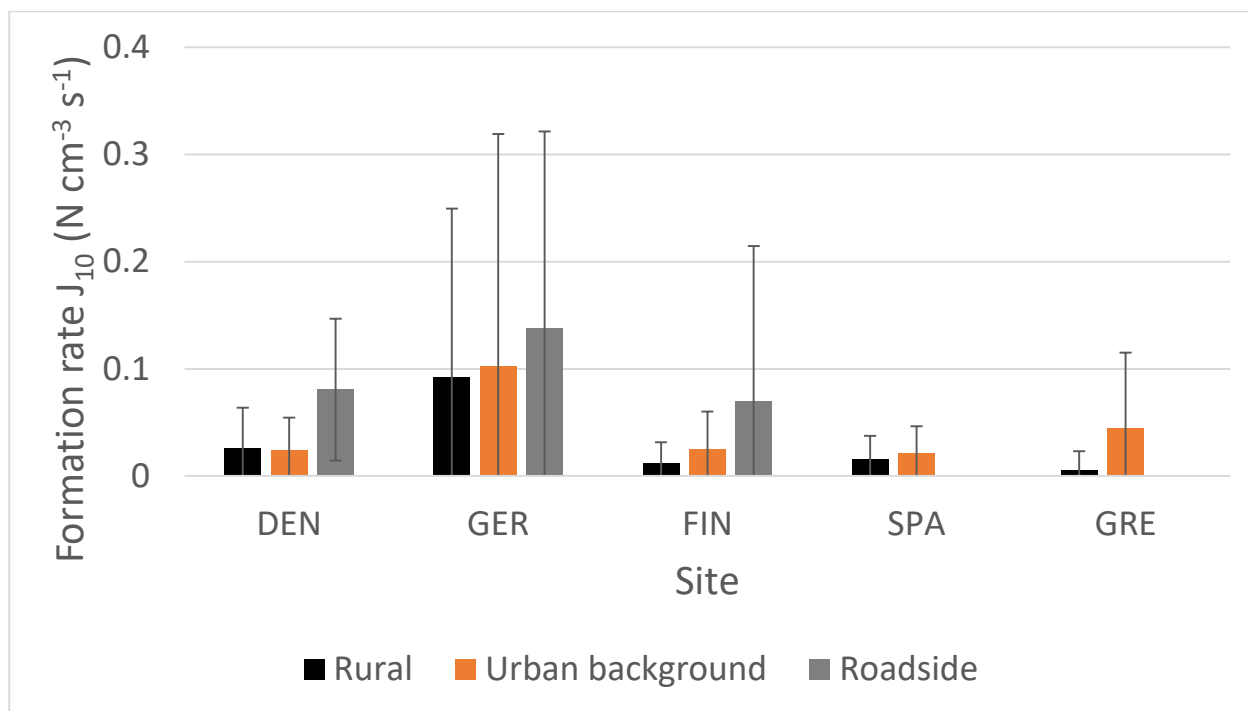
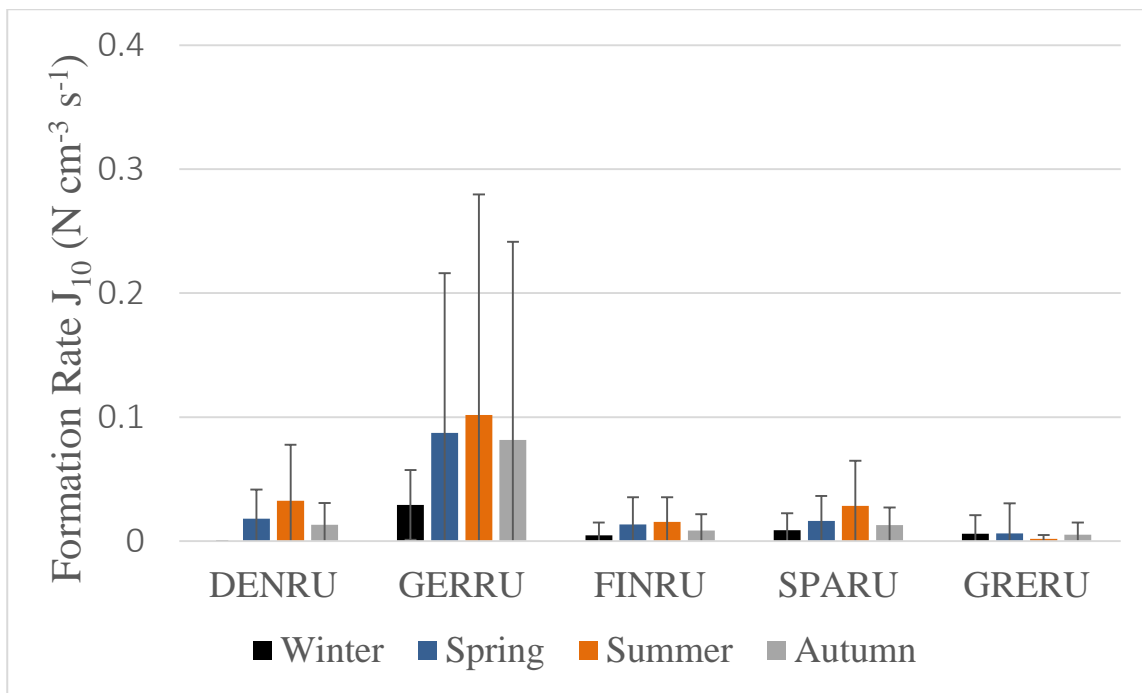
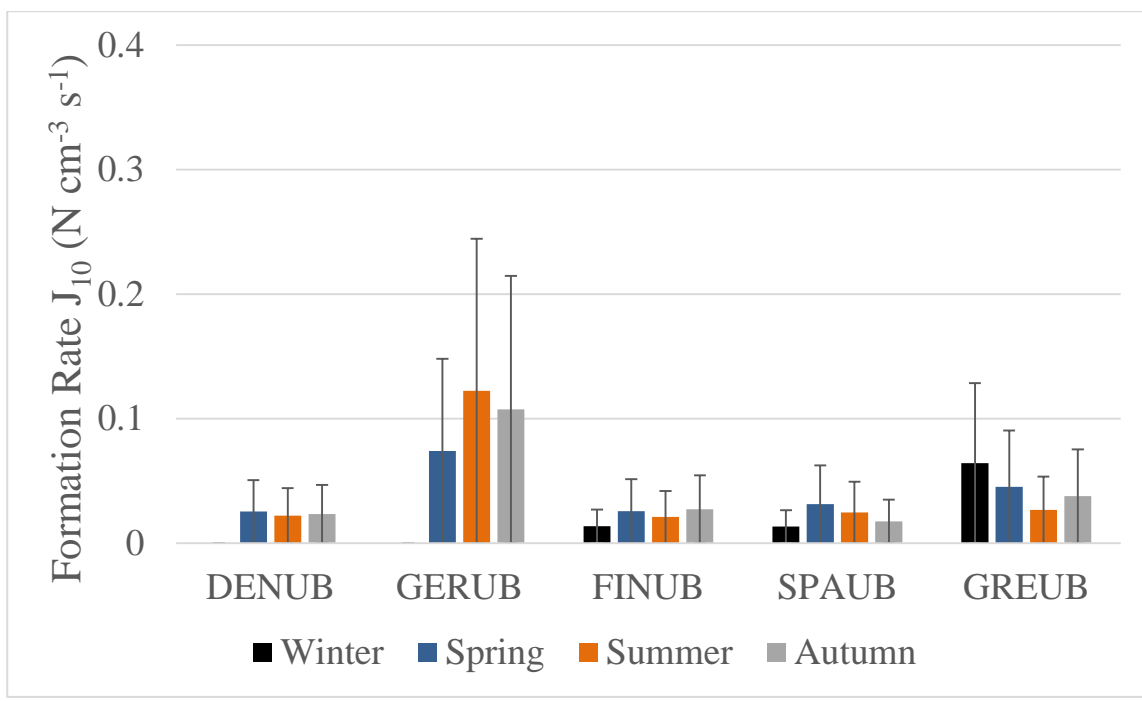


**Figure 6:** Formation rate of 10 nm particles ( $J_{10}$ ) (with standard deviations) during New Particle Formation events at all sites.

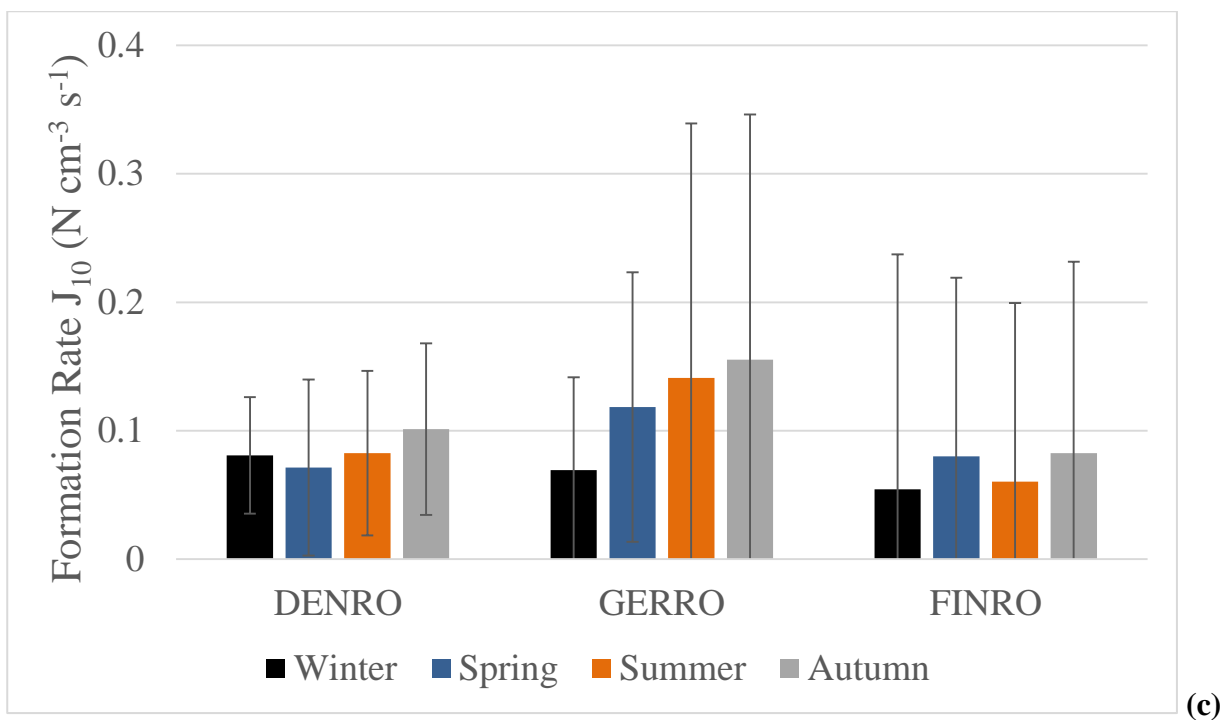
1435



(a)

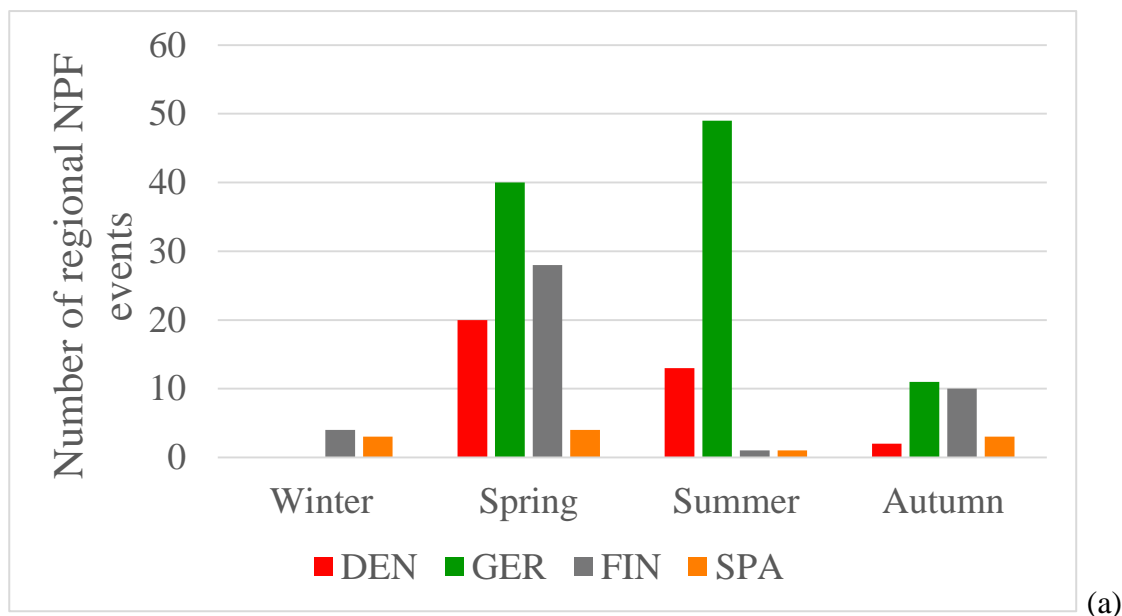


(b)

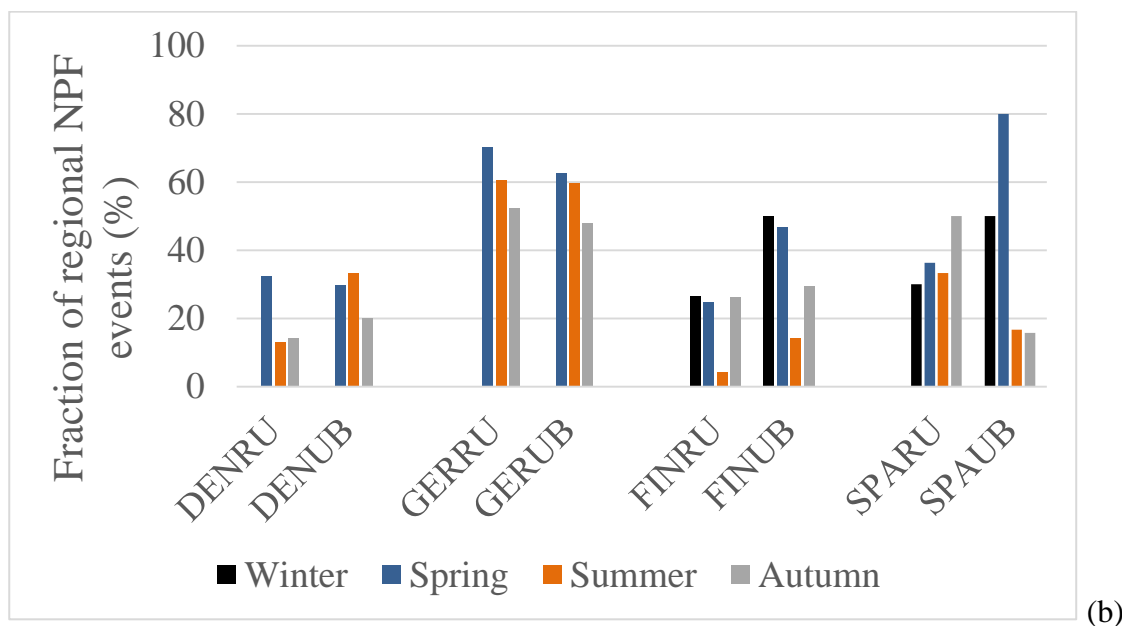


1440 **Figure 7:** Seasonal variation of formation rate of 10 nm particles ( $J_{10}$ ) (with standard deviations) from New Particle Formation events at (a) the rural background, (b) urban background and (c) roadside sites.

1445



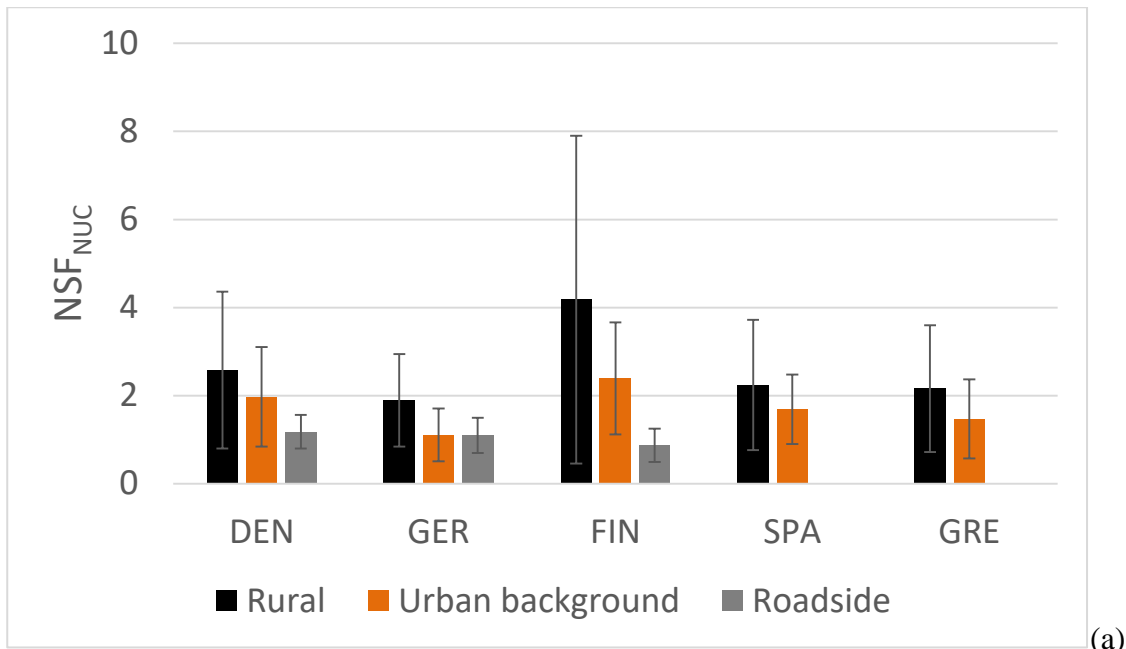
(a)



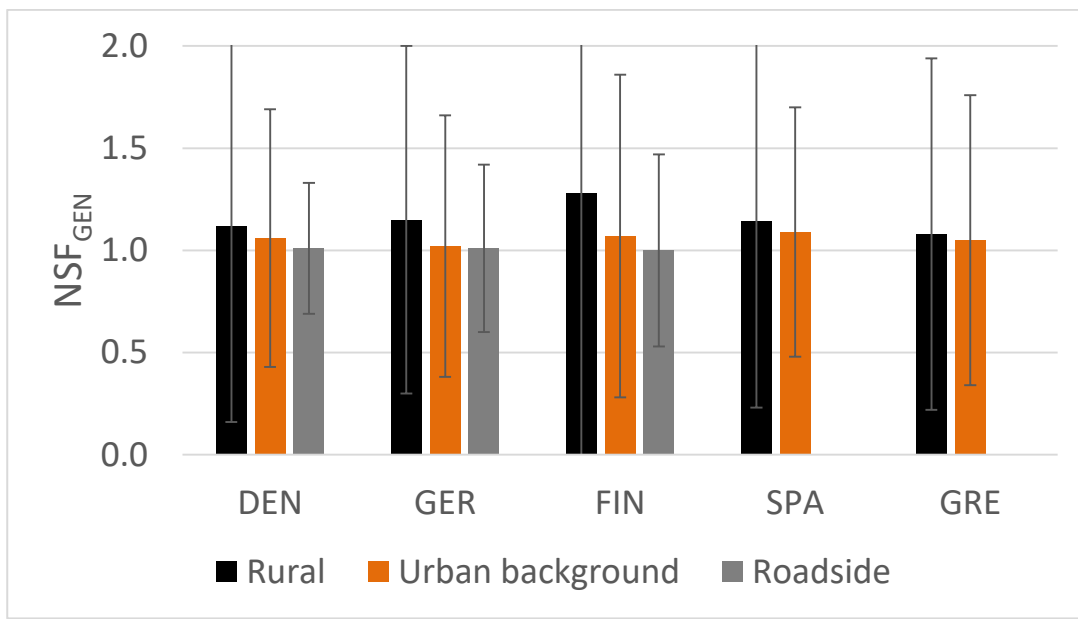
(b)

1450

**Figure 8:** (a) Number of region-wide New Particle Formation events per season and (b) fraction of region-wide events to total New Particle Formation events per season for each site. Region-wide events are defined as those that occur on the same day at both background sites (Rural and Urban background).



(a)



(b)

1455

**Figure 9:** (a)  $NSF_{NUC}$  (average relative increase of ultrafine particles – particles of diameter up to 100 nm) due to New Particle Formation events on event days) and (b)  $NSF_{GEN}$  (average annual relative increase of ultrafine particles due to New Particle Formation events) at all sites.